JACS
JOURNAL OF THE AMERICAN CHEMICAL SOCIETY

ARTICLE

pubs.acs.org/JACS

$[(^{H}L)_2Fe_6(NCMe)_m]^{n+}$ (m = 0, 2, 4, 6; n = −1, 0, 1, 2, 3, 4, 6): An Electron-Transfer Series Featuring Octahedral Fe_6 Clusters Supported by a Hexaamide Ligand Platform

Qinliang Zhao, T. David Harris, and Theodore A. Betley*

Department of Chemistry and Chemical Biology, Harvard University, 12 Oxford Street, Cambridge Massachusetts 02138, United States

Supporting Information

ABSTRACT: Using a trinucleating hexaamide ligand platform, the all-ferrous hexanuclear cluster $(^{H}L)_2Fe_6$ (**1**) is obtained from reaction of 3 equiv of $Fe_2(Mes)_4$ (Mes = 2,4,6-$Me_3C_6H_2$) with 2 equiv of the ligand $(^{H}L)H_6$. Compound **1** was characterized by X-ray diffraction analysis, ^{57}Fe Mössbauer, SQUID magnetometry, mass spectrometry, and combustion analysis, providing evidence for an S = 6 ground state and delocalized electronic structure. The cyclic voltammogram of $[(^{H}L)_2Fe_6]^{n+}$ in acetonitrile reveals a rich redox chemistry, featuring five fully reversible redox events that span six oxidation states ($[(^{H}L)_2Fe_6]^{n+}$, where $n = -1 \rightarrow 4$) within a 1.3 V potential range. Accordingly, each of these species is readily accessed chemically to provide the electron-transfer series $[(^{H}L)_2Fe_6(NCMe)_m][PF_6]_n$ (m = 0, $n = -1$ (**2**); $m = 2$, $n = 1$ (**3**); $m = 4$, $n = 2$ (**4**); $m = 6$, $n = 3$ (**5**); $m = 6$, $n = 4$ (**6**)). Compounds **2**−**6** were isolated and characterized by X-ray diffraction, ^{57}Fe Mössbauer and multinuclear NMR spectroscopy, and combustion analysis. Two-electron oxidation of the tetracationic cluster in **6** by 2 equiv of $[NO]^+$ generates the thermally unstable hexacationic cluster $[(^{H}L)_2Fe_6(NCMe)_m]^{6+}$, which is characterized by NMR and ^{57}Fe Mössbauer spectroscopy. Importantly, several stepwise systematic metrical changes accompany oxidation state changes to the $[Fe_6]$ core, namely *trans* ligation of solvent molecules and variation in Mössbauer spectra, spin ground state, and intracluster Fe−Fe separation. The observed metrical changes are rationalized by considering a qualitative, delocalized molecular orbital description, which provides a set of frontier orbitals populated by Fe 3d electrons.

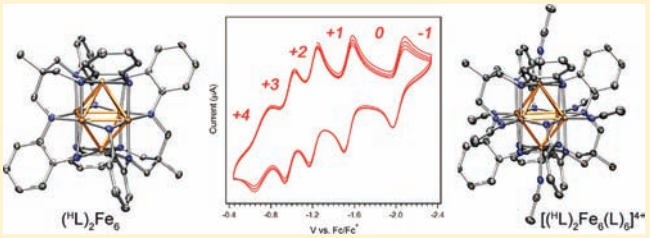

1. INTRODUCTION

Polynuclear molecular complexes have long captivated synthetic chemists, owing to their ability to exhibit a wide range of desirable properties, such as the capacity for stepwise, multielectron redox chemistry, the ability to mediate cooperative reaction chemistry, and access to tunable electronic, magnetic, and photophysical properties. Nature exploits these desirable attributes by employing polynuclear cofactors to effect small-molecule activation in enzymatic pathways. For example, polynuclear assemblies are utilized in the cofactors of nitrogenases to fix atmospheric nitrogen (FeMo, VFe, Fe-only, P-cluster),[1] photosystem II to evolve oxygen from water,[2] and nitrous oxide reductase to degrade higher oxides of nitrogen.[3] While many mechanistic details of these processes remain unresolved, the polynuclear cofactors are hypothesized to aid enzymatic function in mediating multielectron redox processes,[4,5] utilizing multiple metal sites and coordination modes for cooperative substrate binding, stabilization of reactive intermediates,[6] and facilitation of electron transport.[7]

In view of Nature's elegant precedent, coordination chemists have sought to engender expanded redox capabilities by constructing polynuclear transition metal clusters that feature redox-active metal ions and/or ligand scaffolds. Current state-of-the-art synthetic methods often rely on the self-assembly of polynuclear clusters via reaction of metal precursors with suitable bridging ligands that position metal ions close to one another (ca. 3 Å or less) within the cluster. Metal clusters featuring bridging halide,[8] chalcogenide,[7b,c,9−11] alkoxide,[12] imide,[13] and carbonyl[14] ligands are representative of this design strategy, wherein transition metal ions assemble in solution into a broad range of structure types and nuclearities. These systems can often give rise to expanded redox capabilities and stabilize metal clusters over large windows of chemical potential.[15] However, the formation of many clusters often relies on serendipitous reaction pathways. Indeed, such unpredictability of the nuclearity and topology of the resulting clusters often does not permit the rational design of new clusters or facile modification of existing clusters, such that the steric or electronic properties of the cluster cores cannot be readily directed.

One method for enabling the rational design of clusters relies on the employment of rigid, multiatom bridging ligands, such as cyanide[16] or nitrogen-containing heterocycles,[17] to impose limitations on cluster topology and nuclearity. However, such ligands also position intracluster metal ions apart from one another, which often limits cooperative metal−metal interactions,

Received: February 19, 2011
Published: May 11, 2011

   dx.doi.org/10.1021/ja2015845 | J. Am. Chem. Soc. 2011, 133, 8293–8306

especially in the absence of a mixed-valence metal architecture. As an alternative, one can envision use of a single ligand scaffold that features multiple binding pockets, capable of sequestering multiple metal ions in a preconceived proximal space. Toward this end, we have established a family of trinucleating hexaamine-based ligands and their ability to direct the formation of trinuclear iron complexes that demonstrate delocalized redox capabilities in simple electron-transfer processes and cooperative small-molecule activation processes.[18,19] Furthermore, simple perturbations to the ligand scaffold alter the molecular and thus electronic structure of the trinuclear core, giving rise to a wide range of spin states within nominally all-ferrous cores. Encouraged by these results, we sought to employ the trinuclear subunits as building units for higher-nuclearity structures confined within the polyamide framework. Herein, we report the construction of a hexanuclear, octahedral cluster $(^{H}L)_2Fe_6$ via dimerization of two $(^{H}L)Fe_3$ subunits. This cluster shows a large capacity for multisequential, multielectron-transfer processes, wherein the $[Fe_6]^{n+}$ complex is stabilized over eight distinct oxidation states, with six of those redox isomers being structurally characterized. Furthermore, a suite of spectroscopic and other analytical techniques is employed to probe the redox-directed binding of ancillary ligands and metrical changes associated with oxidation of the $[Fe_6]$ core. Finally, these systematic changes to the $[Fe_6]$ core as a function of oxidation state are rationalized through a qualitative delocalized electronic structure model.

2. EXPERIMENTAL SECTION

General Considerations. All manipulations involving metal complexes were carried out using standard Schlenk line or glovebox techniques under a dinitrogen atmosphere. All glassware was oven-dried for a minimum of 10 h and cooled in an evacuated antechamber prior to use in the drybox. Acetonitrile, benzene, diethyl ether, and tetrahydrofuran (THF) were dried and deoxygenated on a Glass Contour System (SG Water USA, Nashua, NH) and stored over 4 Å molecular sieves (Strem) prior to use. Acetonitrile-d_3 was purchased from Cambridge Isotope Laboratories and stored over 4 Å molecular sieves prior to use. Nonhalogenated solvents were typically tested with a standard purple solution of sodium benzophenone ketyl in THF in order to confirm effective oxygen and moisture removal. The compounds $Fe_2(Mes)_4$ (Mes = 2,4,6-$Me_3C_6H_2$)[20] and $MeC(CH_2NHPh\text{-}o\text{-}NH_2)_3$ ($^{H}LH_6$)[18] were prepared according to literature procedures. All other reagents were purchased from commercial vendors and used without further purification unless explicitly stated.

$(^{H}L)_2Fe_6$ (1). To a stirred suspension of $^{H}LH_6$ (0.513 g, 1.31 mmol) in benzene (20 mL) was added a solution of $Fe_2(Mes)_4$ (1.16 g, 1.97 mmol) in a mixture of benzene (20 mL) and pyridine (4 mL), giving a dark brown slurry. The slurry was stirred for 12 h, and the resulting brown precipitate was collected on a medium-porosity fritted glass funnel. The residue was washed with successive aliquots of benzene (3 × 5 mL) and THF (4 × 20 mL) and then dried under vacuum to give **1** (0.680 g, 94%) as a dark brown powder. Crystals suitable for X-ray diffraction studies were obtained by allowing the combined benzene/THF filtrate to stand at room temperature for 2 days. ESI-MS (m/z): $C_{46}H_{48}Fe_6N_{12}^{+}$, 1104.0. Zero-field ^{57}Fe Mössbauer (δ, $|\Delta E_Q|$ (mm/s)): (100 K) 0.48, *1.79* (γ = 0.19 mm/s). Anal. Calcd for $C_{46}H_{48}Fe_6N_{12}$: C, 50.04; H, 4.38; N, 15.22. Found: C, 49.93; H, 4.45; N, 15.40.

$[Na(Et_2O)_2(NCMe)_2][(^{H}L)_2Fe_6]$ (2). To a freshly prepared Na mirror (0.020 g, 0.87 mmol) was added a solution of naphthalene (0.012 g, 0.094 mmol) in THF (6 mL), resulting in a dark green supernatant. The supernatant was stirred for 5 h and then carefully decanted onto a stirred suspension of **1** (0.10 g, 0.091 mmol) in THF (6 mL). The resulting dark brown mixture was stirred for 12 h, and then the THF was removed under vacuum. The remaining brown residue was washed with hexane (4 × 15 mL) and then extracted into MeCN (10 mL). The resulting yellow-brown mixture was filtered through diatomaceous earth, and the dark yellow filtrate was dried under vacuum to give **2** (0.079 g, 79%) as a dark yellow solid. Single crystals, suitable for X-ray diffraction, were obtained by dissolving the brown residue in a 2:1 mixture of MeCN/Et_2O (4 mL), filtering the yellow-brown mixture through diatomaceous earth, and allowing the dark yellow filtrate to stand at −35 °C for 2 days. ^{1}H NMR (CD_3CN, 500 MHz, δ, ppm): 7.35, 3.62, 3.39, 1.93, 1.79, 1.26, 1.11, 0.87. Zero-field ^{57}Fe Mössbauer (δ, $|\Delta E_Q|$ (mm/s)): (100 K) 0.65, *1.03* (γ = 0.30 mm/s) (65% of sample, 35% match metrical parameters for **1**). Anal. Calcd for $C_{58}H_{72}Fe_6N_{14}Na_1O_2$: C, 51.32; H, 5.50; N, 14.45. Found: C, 51.26; H, 5.48; N, 14.43.

$[(^{H}L)_2Fe_6(NCMe)_2]PF_6$ (3). To a solution of **4** (0.042 g, 0.027 mmol) in MeCN (5 mL) was added a solution of Cp_2Co (0.0051 g, 0.027 mmol) in THF (10 mL), giving a dark red solution. Et_2O (30 mL) was added to this solution, resulting in the precipitation of a dark red solid. The solid was washed with Et_2O and hexane until washings were colorless. The solid was dissolved in acetonitrile, filtered through a plug of diatomaceous earth, and concentrated in vacuum to afford a dark red solid (0.034 g, 93%). Single crystals, suitable for X-ray diffraction, were obtained by vapor diffusion of diethyl ether into a concentrated solution of **3** in MeCN, stored at −35 °C. Zero-field ^{57}Fe Mössbauer (δ, $|\Delta E_Q|$ (mm/s)): (100 K) component 1, 0.38, *2.20* (γ = 0.11 mm/s) (54%); component 2, 0.50, *1.93* (γ = 0.26 mm/s) (46%). Anal. Calcd for $C_{50}H_{54}F_6Fe_6N_{14}P$ (**2**): C 45.12, H 4.09, N 14.73. Found: C, 45.03; H, 4.01; N, 14.58.

$[(^{H}L)_2Fe_6(NCMe)_4][PF_6]_2$ (4). To a stirred suspension of **1** (0.200 g, 0.181 mmol) in MeCN (15 mL) was added a solution of $[Cp_2Fe](PF_6)$ (0.120 g, 0.363 mmol) in MeCN (15 mL), giving a dark brown slurry. The slurry was stirred for 12 h to give a dark solution. The solvent was removed under vacuum, and the resulting solid was washed with Et_2O (4 × 15 mL) to remove Cp_2Fe. The dark red residue was extracted into MeCN, filtered through a plug of diatomaceous earth, and dried under vacuum to give 0.255 g (90%) of product. Single crystals, suitable for X-ray diffraction, were obtained by vapor diffusion of diethyl ether into a concentrated solution of **4** in MeCN, stored at −35 °C. ^{1}H NMR (CD_3CN, 400 MHz, δ, ppm): 15.9 (br s, N−*H*), 7.28 (br s, aromatic C−*H*), 6.32 (br s, aromatic C−*H*), 5.58 (br s, aromatic C−*H*), 1.96 (s, NC−C*H*$_3$), 0.81 (s, C−C*H*$_3$), −12.6 (br s, C−C*H*$_a$H$_b$−N), −13.7 (br s, C−CH$_a$*H*$_b$−N). Zero-field ^{57}Fe Mössbauer (δ, $|\Delta E_Q|$ (mm/s)): (100 K) component 1, 0.35, *2.68* (γ = 0.19 mm/s) (33%); component 2, 0.46, *2.18* (γ = 0.19 mm/s) (67%). Anal. Calcd for $C_{54}H_{60}F_{12}Fe_6N_{16}P_2$: C, 41.62; H, 3.88; N, 14.38. Found: C, 41.48; H, 3.97; N, 14.26.

$[(^{H}L)_2Fe_6(NCMe)_6][PF_6]_3$ (5). To a stirred suspension of **1** (0.200 g, 0.181 mmol) in MeCN (15 mL) was added a solution of $[Cp_2Fe](PF_6)$ (0.180 g, 0.544 mmol) in MeCN (15 mL), giving a dark brown slurry. The slurry was stirred for 12 h to give a dark solution. The solvent was removed under vacuum, and the resulting solid was washing with Et_2O (4 × 15 mL) to remove Cp_2Fe. The dark brown residue was extracted into MeCN, filtered through a plug of diatomaceous earth, and dried under vacuum to give 0.265 g (82%) of product. Single crystals, suitable for X-ray diffraction, were obtained by vapor diffusion of diethyl ether into a concentrated solution of **5** in MeCN, stored at −35 °C. ^{1}H NMR (CD_3CN, 400 MHz, δ, ppm): 9.29 (br s, N−*H*), 7.56 (br s, aromatic C−*H*), 7.34 (br s, aromatic C−*H*), 7.10 (br s, aromatic C−*H*), 6.64 (br s, aromatic C−*H*), 1.96 (s, NC−C*H*$_3$), 0.86 (br s, C−C*H*$_3$), −6.22 (br s, C−C*H*$_a$H$_b$−N), −7.32 (br s, C−CH$_a$*H*$_b$−N). Zero-field ^{57}Fe Mössbauer (δ, $|\Delta E_Q|$ (mm/s)): (100 K) 0.42, *2.52* (γ = 0.19 mm/s). Anal. Calcd for $C_{58}H_{66}F_{18}Fe_6N_{18}P_3$: C, 39.02; H, 3.73; N, 14.12. Found: C, 38.87; H, 3.62; N, 14.03.

$[(^{H}L)_2Fe_6(NCMe)_6][PF_6]_4$ (6). To a stirred suspension of **1** (0.200 g, 0.181 mmol) in MeCN (15 mL) was added a solution of $[Cp_2Fe](PF_6)$ (0.246 g, 0.743 mmol) in CH_3CN (15 mL), giving a dark brown slurry. The slurry was stirred for 12 h to give a dark solution. The solvent was removed under vacuum, and the resulting solid was washed with Et_2O (4 × 15 mL) to remove Cp_2Fe, followed by THF (10 × 20 mL) to remove excess $[Cp_2Fe](PF_6)$. The dark yellow residue was extracted into MeCN, filtered through a plug of diatomaceous earth, and then dried under vacuum to give 0.304 g (87%) of product. Single crystals, suitable for X-ray diffraction, were obtained by vapor diffusion of diethyl ether into a concentrated solution of **6** in MeCN at room temperature left to stand overnight. ^{1}H NMR (CD_3CN, 400 MHz, δ, ppm): 7.73 (d, 3H, aromatic C−*H*), 7.43 (t, 3H, aromatic C−*H*), 7.19 (t, 3H, aromatic C−*H*), 6.77 (d, 3H, aromatic C−*H*), 5.69 (s, 3H, N−*H*), 2.96 (d, 3H, C−C*H*$_a$H$_b$−N), 2.35 (d, 3H, C−CH$_a$*H*$_b$−N); 1.96 (s, NC−C*H*$_3$), 0.97 (s, 3H, C−C*H*$_3$). ^{13}C{^{1}H} NMR (CD_3CN, 500 MHz, δ, ppm): 157, 153, 128, 128, 119, 118, 66, 34, 24, 0.59. Zero-field ^{57}Fe Mössbauer (δ, $|\Delta E_Q|$ (mm/s)): (100 K) 0.40, *2.50* (γ = 0.18 mm/s). Anal. Calcd for $C_{58}H_{66}F_{24}Fe_6N_{18}P_4$: C, 36.09; H, 3.45; N, 13.06. Found: C, 35.91; H, 3.40; N, 13.14.

$[(^{H}L)_2Fe_6(NCCH_3)_6][PF_6]_6$ (7). To a frozen solution of **6** (0.025 g, 0.013 mmol) in MeCN (1 mL) standing at ca. −77 °C was added a solution of $[NO]PF_6$ (0.0091 g, 0.052 mmol) in MeCN (1 mL). The resulting frozen mixture was allowed to thaw at ambient temperature. Immediately upon melting, the resulting dark brown solution was dried under vacuum to give a highly thermally unstable brown residue. Due to the instability of the compound, residual $[NO]PF_6$ could not be separated. As such, no product yield or elemental analysis is reported. ^{1}H NMR (CD_3CN, 400 MHz, δ, ppm): 18.2 (s, N−*H*), 11.6 (s, aromatic C−*H*), 9.05 (s, aromatic C−*H*), 7.18 (s, aromatic C−*H*), 6.85 (s, aromatic C−*H*), 3.84 (s, C−C*H*$_a$H$_b$−N), 2.14 (s, C−C*H*$_3$), 1.96 (s, NC−C*H*$_3$), −9.62 (s, C−CH$_a$*H*$_b$−N). Zero-field ^{57}Fe Mössbauer (δ, $|\Delta E_Q|$ (mm/s)): (100 K) 0.37, *2.54* (γ = 0.19 mm/s).

X-ray Structure Determinations. Single crystals suitable for X-ray analysis were coated with deoxygenated Paratone-N oil and mounted on Kaptan loops. Data for compounds **1**−**6** were collected at 100 K on an APEX II CCD or APEX II DUO single-crystal diffractometer. None of the crystals showed significant decay during data collection. Raw data were integrated and corrected for Lorentz and polarization effects using Bruker APEX2 v. 2009.1.[21] Absorption corrections were applied using SADABS.[22] Space group assignments were determined by examination of systematic absences, E-statistics, and successive refinement of the structures. The program PLATON[23] was employed to confirm the absence of higher symmetry for any of the crystals. The positions of the heavy atoms were determined using direct methods using the program SHELXTL.[24] Subsequent cycles of least-squares refinement followed by difference Fourier syntheses revealed the positions of the remaining non-hydrogen atoms. Non-hydrogen atoms were refined with anisotropic displacement parameters, and hydrogen atoms were added in idealized positions. Crystallographic data for **1**−**6** are given in the Supporting Information, Table S1.

Magnetic Susceptibility Measurements. Magnetic data for **1** and **5** were collected using a Quantum Design MPMS-5S SQUID magnetometer. Measurements were obtained for microcrystalline powders restrained in a frozen eicosane matrix within gelatin capsules. Samples were prepared under a dinitrogen atmosphere. Direct current (dc) magnetic susceptibility measurements were collected in the temperature range 2−300 K under an applied dc field of 1 T. All data were corrected for core diamagnetism of the sample, estimated using Pascal's constants, in addition to contributions from the sample holder and eicosane. Note that magnetic data were not collected for compounds **2**, **3**, **4**, and **7** due to compound instability.

Other Physical Measurements. Elemental analyses were performed by Complete Analysis Laboratories, Inc. (Parsippany, NJ) or Robertson Microlit Laboratories (Madison, NJ). ^{1}H NMR spectra were recorded on a Varian Mercury 400 NMR spectrometer with chemical shifts (δ ppm) referenced to residual NMR solvent. Solution magnetic susceptibilities were determined by Evans's method[25] using hexamethyldisiloxane as an internal reference. Low-resolution ESI-MS of air-sensitive samples was obtained on an Agilent 6120 Quadrupole LC/MS with sample introduced by direct injection of a THF solution using an airtight syringe. Zero-field ^{57}Fe Mössbauer spectra were measured with a constant acceleration spectrometer (SEE Co., Minneapolis, MN). Isomer shifts are quoted relative to Fe metal at room temperature. Data were analyzed with WMOSS software (Web Research Corp., Edina, MN).

3. RESULTS AND DISCUSSION

3.1. Synthesis and Characterization of $(^{H}L)_2Fe_6$. We recently reported the synthesis of a hexaamine ligand scaffold, $MeC(CH_2NHPh\text{-}o\text{-}NH_2)_3$ ($^{H}LH_6$), that readily binds three divalent metal ions within a proximal trigonal planar arrangement (e.g., $(^{H}L)Fe_3(PMe_2R)_3$).[18] The metal complexes are formed via a transamination reaction from an organometallic precursor (e.g., $Fe_2(Mes)_4$; Mes = 2,4,6-$Me_3C_6H_2$),[20] wherein the two amine groups on each *o*-phenylenediamine arm of the ligand are both deprotonated to give the formally hexa-anionic ligand $[^{H}L]^{6-}$. Formation of the trinuclear complexes requires the presence of a strong σ-donating tertiary phosphine (e.g., PMe_2R, R = Me, Ph) to bind each of the metal centers. In the absence of the phosphine co-ligand, however, the transamination reaction yields a species quite unlike the highly soluble trinuclear complexes. Indeed, reaction of $Fe_2(Mes)_4$ with $^{H}LH_6$ in a 3:2 stoichiometric ratio in a mixture of benzene and pyridine rapidly produces a dark brown precipitate (see Scheme 1). During the course of the reaction, ^{1}H NMR analysis confirms consumption of the organometallic precursor, though the new product exhibits no observable proton resonances. Electrospray mass spectrometry on the filtered reaction mixture reveals a parent ion with a mass/charge ratio of 1104 *m*/*z*, matching the molecular weight and isotope pattern calculated for a species of formula $(^{H}L)_2Fe_6$ (see Supporting Information, Figure S1). Despite the marked insolubility of this material, crystals suitable for a single crystal X-ray diffraction study were grown from the crude reaction mixture at room temperature, providing structural confirmation of the cluster compound $(^{H}L)_2Fe_6$ (**1**, see Figure 1a). Compound **1** crystallizes in the trigonal space group $R\bar{3}$, where the asymmetric unit features a single Fe center that resides on a site of S_6 symmetry. Overall, the cluster is comprised of an edge-bridged octahedral arrangement of Fe centers, with twelve amide nitrogen atoms situated at the edge vertices. Neglecting Fe−Fe interactions, each iron is bound by four ligand amide nitrogen atoms (two N1, two N2, see Figure 1b) to form a square plane. Additionally, each Fe center features four closest neighbor Fe ions at distances of 2.5963(17) and 2.5981(15) Å within the octahedral core. The Fe−Fe distances are expanded from the neutral compounds $(^{H}L)Fe_3(PMe_2R)_3$ (2.299(2) Å mean distance) and cationic complex $(^{H}L)Fe_3(PMe_3)_3$ (2.271(1) Å), where the Fe centers are capped by phosphine ligands,[18] but are within the range where Fe−Fe bonding interactions have previously been reported in other molecules.[26] To our knowledge, compound **1** is the only coordination compound featuring an edge-bridged octahedron of Fe ions not supported by bridging carbonyl[14,27] or chalcogenide (e.g., S, Te) ligands[11o−t,28] or interstitial oxygen atoms.[29]

Scheme 1. Synthesis of the Hexanuclear Cluster Compound $(^{H}L)_2Fe_6$ (1) and the Chemical Oxidation Products Using Ferrocenium Hexafluorophosphate $[Cp_2Fe]PF_6$ as the Stoichiometric Oxidant

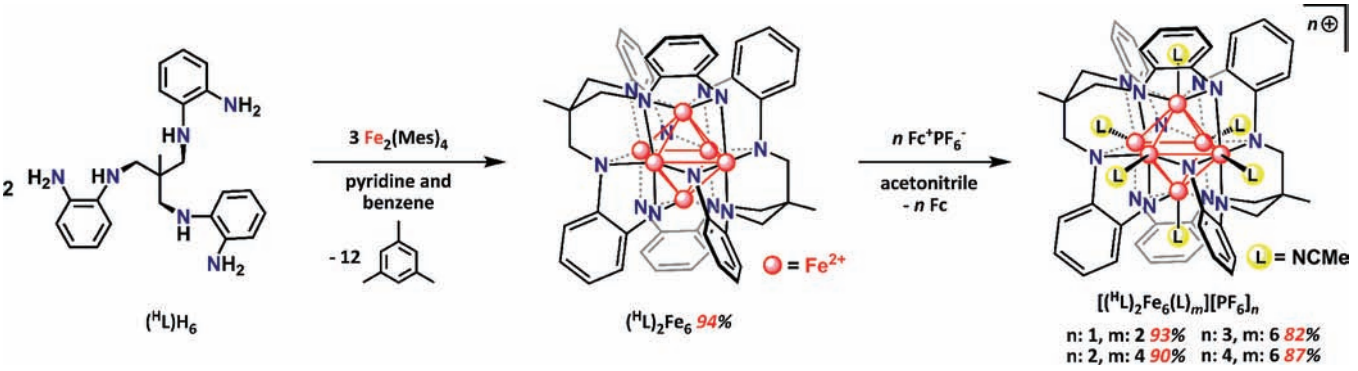

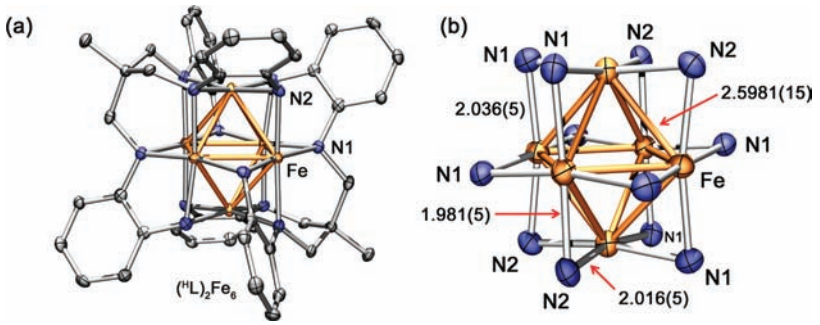

Figure 1. Solid-state molecular structure of **1** obtained at 100 K (a); expanded view of $[Fe_6N_{12}]$ core in **1** (b).

3.2. Redox Behavior of $(^{H}L)_2Fe_6$: Cyclic Voltammetry. The insolubility of **1** precludes satisfactory electrochemical analysis for the complex. However, reaction of complex **1** with 3 equiv of ferrocenium hexafluorophosphate ($[Cp_2Fe]PF_6$) in acetonitrile yields the soluble tricationic cluster $[(^{H}L)_2Fe_6(NCMe)_6]^{3+}$ (*vide infra*) and 3 equiv of ferrocene. Cyclic voltammetry on an acetonitrile solution containing $[(^{H}L)_2Fe_6(NCMe)_6]^{3+}$ (0.1 M $(Bu_4N)PF_6$; scan rate of 0.05 V/s) reveals a rich sequence of fully reversible one-electron redox events (see Figure 2). Specifically, scanning cathodically from a starting potential of −0.475 V (vs Cp_2Fe), the cyclic voltammogram shows five fully reversible, one-electron processes, with $E_{1/2}$ (V) = −0.72, −0.99, −1.22, −1.55, −2.04 V and $\Delta E_{A\text{-}C,avg}$ = 83 mV, suggesting the following electron-transfer series:

$$[Fe_6]^{-} \overset{-2.04V}{\rightleftharpoons} [Fe_6]^{0} \overset{-1.55V}{\rightleftharpoons} [Fe_6]^{+} \overset{-1.22V}{\rightleftharpoons} [Fe_6]^{2+} \overset{-0.99V}{\rightleftharpoons} [Fe_6]^{3+} \overset{-0.72V}{\rightleftharpoons} [Fe_6]^{4+}$$

The inferred resting state potential for **1** is approximately −1.8 V versus an internal ferrocene standard, comparable to the related tri-iron complexes.[18] The $[(^{H}L)_2Fe_6]^{n+}$ cluster represents a unique electron-transfer series, in that six oxidation states are observed in a potential window spanning only 1.3 V. While the separation between the anionic species $[Fe_6]^{-}$ and the neutral species $[Fe_6]^{0}$ is 0.49 V, the subsequent consecutive oxidations occur in a much more narrow potential range, where $\Delta E_{1/2}$ ($[Fe_6]^{(n+1)}-[Fe_6]^{n}$, n = 1−4) = 0.33, 0.23, 0.27 V). The presence of fully resolved, one-electron redox processes in the cyclic voltammogram of $[(^{H}L)_2Fe_6(NCMe)_6]^{3+}$ is indicative of strong

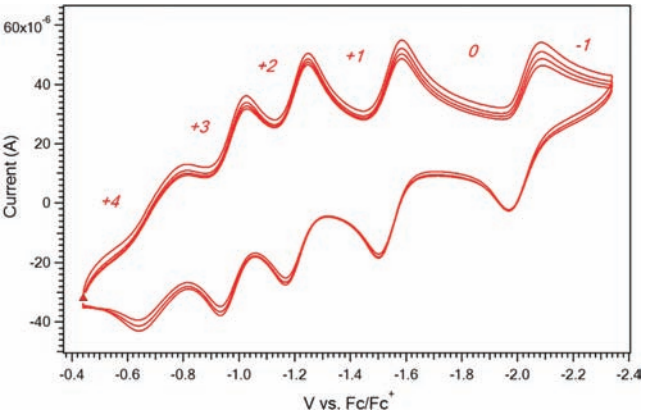

Figure 2. Cyclic voltammogram of $[(^{H}L)_2Fe_6(NCMe)_6]^{3+}$ (glassy C working electrode, 0.1 M Bu_4NPF_6, scan rate 0.05 V/s in acetonitrile, referenced to ferrocene$^{0/+}$).

electronic interaction between the Fe ions within Fe_6 core. Indeed, the separation of adjacent redox events reflects the stabilization energy imparted to the molecule by electron delocalization,[30,31] suggesting a minimal reorganization penalty required as the core traverses the redox sequence.[15a]

The redox flexibility displayed by the $[Fe_6]$ electron-transfer series is exceedingly rare among molecular compounds. Fullerenes and their derivatives,[32] tungsten chloride clusters,[33] polyoxometalate complexes,[29] and metal complexes bearing

dx.doi.org/10.1021/ja2015845 |J. Am. Chem. Soc. 2011, 133, 8293–8306

multiple redox-active ligands[34] can sometimes provide access to a similarly large number of resolvable redox processes. Additionally, iron−sulfur clusters[7b,35] can demonstrate stabilization across a number of oxidation states, such as in the face-capped octahedral clusters $[Fe_6S_8(PEt_3)_6]^{n+}$.[11r,36] This cluster electron-transfer series shows four reversible redox waves across a potential window of 2.4 V, with five of the discrete cluster oxidation states having been isolated and structurally characterized.[11r] However, the potential ranges needed to observe such a litany of redox events in these examples typically span over nearly 2 V, a much larger range than that required in the present case.

3.3. Redox Behavior of $(^{H}L)_2Fe_6$: Chemical Redox. Chemically, complex **1** can be reduced using a single equivalent of sodium naphthalenide ($Na[C_{10}H_8]$) in THF, followed by crystallization from a mixture of acetonitrile and diethyl ether, to cleanly afford the yellow, anionic cluster compound $[Na(OEt_2)_2(NCMe)_2][(^{H}L)_2Fe_6]$ (**2**). Upon standing at room temperature in THF, solutions of **2** will convert to the neutral **1** and precipitate from solution as a brown solid over the course of hours. Storing **2** as a solid or in THF solution at −35 °C maintains the yellow color characteristic of **2** and prevents oxidation over a period of days. Chemical oxidation of **1** can be effected by reaction with stoichiometric equivalents (n) of the one-electron oxidant $[Cp_2Fe]PF_6$ to cleanly afford $[(^{H}L)_2Fe_6(NCMe)_4][PF_6]_2$ (**4**, n = 2, 90%), $[(^{H}L)_2Fe_6(NCMe)_6][PF_6]_3$ (**5**, n = 3, 82%), or $[(^{H}L)_2Fe_6(NCMe_3)_6][PF_6]_4$ (**6**, n = 4, 87%, see Scheme 1). Owing to the insolubility of **1**, attempts to isolate the singly oxidized material using one equivalent of oxidant invariably gave equimolar mixtures of neutral **1** and dicationic cluster-containing **4**, presumably the result of overoxidation of the monocationic cluster upon dissolution. Rather, a one-electron reduction of **4** can be effected using a single equivalent of cobaltacene (Cp_2Co) in acetonitrile to afford the monocationic cluster compound $[(^{H}L)_2Fe_6(NCMe)_2][PF_6]$ (**3**, 93%):

$$\underset{(4)}{[(^{H}L)_2Fe_6(NCMe)_4][PF_6]_2} \xrightarrow[-[Cp_2Co][PF_6]]{Cp_2Co} \underset{(3)}{[(^{H}L)_2Fe_6(NCMe)_2][PF_6]} \quad (1)$$

The cationic cluster compounds **3**−**6** are readily soluble in acetonitrile, in which diagnostic ^{1}H NMR spectra were obtained (see Supporting Information, Figures S2−S5). Compounds **3**−**5** exhibit paramagnetically shifted and significantly broadened ^{1}H resonances, yet all eight distinct protons are observable for both **4** and **5**. The spectrum for **3** is sufficiently broadened, such that only the diastereotopic methylene resonances are visible at −21 ppm. The tetracationic cluster compound **6** displays an ^{1}H spectrum that is consistent with a diamagnetic species (S = 0, see Supporting Information, Figure S4), featuring all eight proton resonances between 0 and 8 ppm, and a fully resolved ^{13}C spectrum.

The cyclic voltammetry studies on $[(^{H}L)_2Fe_6(NCMe)_6]^{3+}$ suggest that oxidation of the cluster core is anodically limited to the tetracationic state. Accordingly, utilizing $[Cp_2Fe]^+$ as an oxidant, the tetracationic cluster compound **6** is the most oxidized species that can be obtained chemically, even when the oxidant is present in excess. Nevertheless, reaction of **6** with the stronger oxidant $[NO]PF_6$ in acetonitrile-d_3 indicates that further oxidation of the cluster is possible. Indeed, treatment of **6** with 2 equiv of $[NO]PF_6$ renders a new paramagnetically shifted ^{1}H spectrum, distinct from **6** but clearly showing all eight resonances expected for an intact cluster (see Supporting Information, Figure S5). We tentatively assign this new species as the hexacationic cluster $[(^{H}L)_2Fe_6(NCMe)_6]^{6+}$, contained within the compound $[(^{H}L)_2Fe_6(NCMe)_6](PF_6)_6$ (**7**, eq 2). Despite the spectroscopic observation of this species, compound **7** is thermally unstable and will revert back to the tetracationic cluster in acetonitrile solution over a period of hours (half-life of ca. 90 min, see Supporting Information, Figure S6), with some concomitant decomposition apparent by ^{1}H NMR. As such, this instability has thus far precluded structural confirmation of the nominally all-ferric cluster.

$$\underset{(6)}{[(^{H}L)_2Fe_6(NCMe)_6][PF_6]_4} \xrightarrow[-2NO]{2[NO]^+[PF_6]^-} \underset{(7)}{[(^{H}L)_2Fe_6(NCMe)_6][PF_6]_6} \quad (2)$$

3.4. Structures of Electron-Transfer Series. The anionic cluster compound **2** and cationic cluster compounds **3**−**6** were crystallized from vapor diffusion of diethyl ether into concentrated solutions of each compound in acetonitrile stored at either −35 °C (**2**−**5**) or ambient temperature (**6**). Depictions of the solid-state molecular structures for complexes **2**−**6** are provided in Figure 3a−e. A comparison of the structures reveals several discernible trends. Most notably, oxidation is associated with stepwise binding of solvent molecules by the Fe centers. In both neutral **1** and anionic cluster compound **2**, the Fe_6 core is bare of any bound exogenous acetonitrile ligands, such that each Fe center resides in the square planar coordination environment described above. However, in monocationic cluster compound **3**, two trans-disposed Fe centers each loosely binds one acetonitrile ligand at the open apical position, with a mean $Fe-N_{NCMe}$ distance of 2.309(18) Å, such that those two Fe centers now feature local square pyramidal coordination. Subsequently, four equatorial Fe centers in dicationic cluster compound **4** each bind an acetonitrile ligand, here more tightly, with a mean $Fe-N_{NCMe}$ distance of 2.007(4) Å. Finally, upon oxidation to tricationic cluster compound **5**, all six Fe centers bind acetonitrile ligands (mean $Fe-N_{NCMe}$ of 2.065(7) Å) and further oxidation to tetracationic cluster compound **6** provides a similar $Fe_6(NCMe)_6$ core (mean $Fe-N_{NCMe}$ of 1.981(3) Å).

In addition to the redox-directed solvent binding, each subsequent oxidation of the $[Fe_6]$ core leads to changes in the average Fe−Fe separation and thus Fe_6 core volume (see Tables 1 and 2). Upon moving from anionic cluster compound **2** to neutral **1**, the mean Fe−Fe distance increases from 2.5804(11) to 2.5972(17) Å. Further, moving stepwise from neutral **1** to tricationic cluster compound **5**, the mean Fe−Fe distance undergoes a stepwise linear increase from 2.5972(17) to 2.7040(13) Å (see Figure 4). In contrast, moving from tricationic cluster compound **4** to tetracationic cluster compound **5** results in a contraction of the mean Fe−Fe separation, from 2.7040(13) to 2.6907(8) Å. These trends are also visible across the series **1**−**6** in the volume subtended by the $[Fe_6]$ octahedral core, which provides a more sensitive measure of structural variation. Notably, the volume of space occupied by the tricationic cluster in **5** (9.321(4) Å^3) represents a 15% increase over that observed for the anionic cluster in **2** (8.116(4) Å^3).

3.5. Mössbauer Spectroscopy. To probe the electronic structure of the Fe_6 cluster and how it is perturbed across the redox series, zero-field ^{57}Fe Mössbauer analysis (see Figures 5 and 6) was carried out on **1**−**7** (see Table 3). The spectrum

dx.doi.org/10.1021/ja2015845 |J. Am. Chem. Soc. 2011, 133, 8293–8306

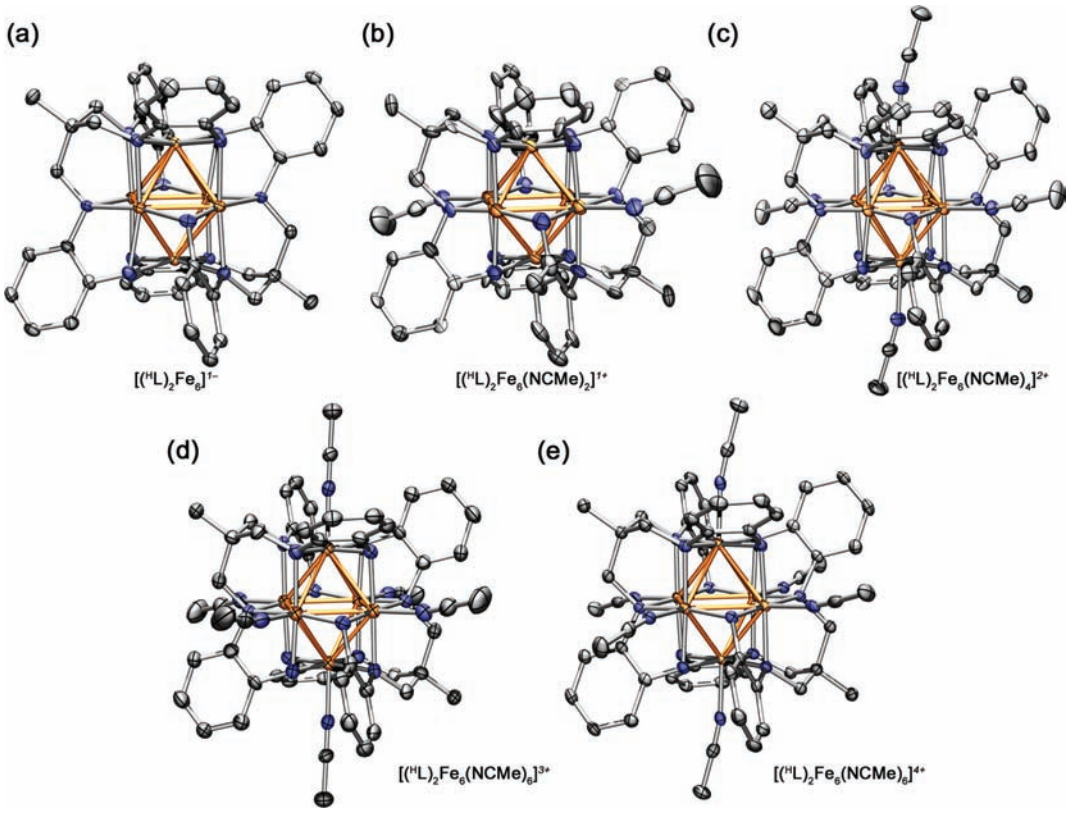

Figure 3. Solid-state molecular structures obtained at 100 K for $[(^{H}L)_2Fe_6]^{-}$, as observed in **2** (a); $[(^{H}L)_2Fe_6(NCMe)_2]^{+}$, as observed in **3** (b); $[(^{H}L)_2Fe_6(NCMe)_4]^{2+}$, as observed in **4** (c); $[(^{H}L)_2Fe_6(NCMe)_6]^{3+}$, as observed in **5** (d); and $[(^{H}L)_2Fe_6(NCMe)_6]^{4+}$, as observed in **6** (e) with the thermal ellipsoids set at the 50% probability level. Orange, blue, and black ellipsoids represent Fe, N, and C atoms, respectively; hydrogen atoms are omitted for clarity.

Table 1. Structural Metrics for Complexes 1−6

compound		Fe−Fe_{avg} (Å)	V (Å^3)
$(^{H}L)_2Fe_6$	**1**	2.5972(18)	8.258(3)
$[Na(Et_2O)_2(NCMe)_2][(^{H}L)_2Fe_6]$	**2**	2.5804(11)	8.116(4)
$[(^{H}L)_2Fe_6(NCMe)_2][PF_6]$	**3**	2.655(6)	8.808(8)
$[(^{H}L)_2Fe_6(NCMe)_4][PF_6]_2$	**4**	2.6877(11)	9.166(3)
$[(^{H}L)_2Fe_6(NCMe)_6][PF_6]_3$	**5**	2.7040(13)	9.321(4)
$[(^{H}L)_2Fe_6(NCMe)_6][PF_6]_4$	**6**	2.6907(8)	9.187(1)

collected for compound **1**, shown in Figure 5b, features a single, symmetric quadrupole doublet with an isomer shift and quadrupole splitting of δ, $|\Delta E_Q|$ (mm/s) = 0.48, *1.79*, respectively, indicative of a single iron coordination environment within the complex.

In contrast to **1**, the data for anionic cluster compound **2** show two quadrupole doublets, with spectral fits revealing 65% of the sample exhibiting parameters of δ, $|\Delta E_Q|$ (mm/s) = 0.65, *1.03*, and 35% of the sample with δ, $|\Delta E_Q|$ (mm/s) = 0.48, *1.79*. Note, however, that the minor component matches exactly to the metrical parameters of **1**. Most likely, the presence of **1** in this sample results from the facile oxidation of **2** and occurs invariably during the Mössbauer sample preparation. In support of this hypothesis, separate data sets collected for samples of **2** give varying amounts of each spectral component. Compounds **3** and **4**, containing the mono- and dicationic clusters, respectively, each display a spectral profile that is best fit as a composite of two quadrupole doublets. This asymmetry is reflective of the reduction in $[Fe_6N_{12}(NCMe)_m]$ core symmetry from O_h to D_{4h} upon oxidation from the neutral cluster. Specifically, the spectrum of **3** can be fit to give the following parameters: δ, $|\Delta E_Q|$ (mm/s) component 1, 0.38, *2.20* (54%), component 2, 0.50, *1.93* (46%)While the anticipated 2:1 ratio for the four- to five-coordinate Fe sites is not exactly reproduced by the spectral fits, the four-coordinate iron sites show a more pronounced dependence of isomer shift on oxidation state than do the acetonitrile-bound, five-coordinate iron centers, as observed across the entire redox series (see below and Figure 6). Likewise, the spectrum of compound **4** is best modeled as two quadrupole doublets in a 2:1 ratio: δ, $|\Delta E_Q|$ (mm/s) component 1, 0.35, *2.68* (33%), component 2, 0.46, *2.18* (67%). Note that both components assume lower isomer shifts in moving from **1** to **3** to **4**, a result of the core oxidation state increase. Again, the four-coordinate iron sites exhibit a lower isomer shift (component 1) than the electrostatically buttressed, acetonitrile-bound Fe center (component 2). While compounds **3** and **4** feature asymmetric spectral profiles, reflective of the presence of two distinct Fe coordination environments in each species, the more symmetric clusters in compounds **5**−**7** all exhibit a single, symmetric quadrupole doublet, indicative of a single electronic environment within each Fe_6 core. This observation is noteworthy, as it demonstrates a delocalized electronic structure for the Fe_6 core on the time scale of the Larmor precession frequency of the iron-57 nuclear magnetic moment (ca. 0.01 μs). Further, successive removal of electrons

Table 2. Selected Mean Interatomic Distances (Å) for Compounds 1−6

	compound					
	1	**2**	**3**	**4**	**5**	**6**
Fe1−Fe2	2.5963(17)	2.6012(11)	2.638(4)	2.6412(10)	2.7143(19)	2.6734(7)
Fe1−Fe3	2.5963(17)	2.5857(10)	2.720(4)	2.6662(10)	2.7144(17)	2.7126(7)
Fe1−Fe2′	2.5981(15)	2.5818(11)	2.571(4)	2.6532(10)	2.6779(19)	2.6978(6)
Fe1−Fe3′	2.5981(15)	2.5598(9)	2.713(4)	2.6344(9)	2.7047(18)	2.6744(7)
Fe2−Fe3	2.5963(17)	2.5887(10)	2.640(4)	2.7743(10)	2.7209(19)	2.7094(7)
Fe2−Fe3′	2.5981(15)	2.5652(10)	2.649(4)	2.7571(9)	2.6920(18)	2.6768(7)
Fe(1)−L(1)			2.309(18)	2.012(4)	2.074(8)	1.968(2)
Fe(2)−L(2)				2.001(4)	2.098(10)	1.993(3)
Fe(3)−L(3)					1.998(7)	1.983(2)
Fe(1)−N(1)	2.036(5)	2.079(3)	2.012(15)	1.981(4)	1.975(6)	1.970(2)
Fe(1)−N(3)	2.037(5)	2.069(3)	2.028(15)	1.983(4)	2.005(7)	1.984(2)
Fe(1)−N(4)	2.016(5)	2.021(3)	1.984(15)	1.961(4)	1.927(7)	1.917(2)
Fe(1)−N(5)	1.981(5)	2.086(3)	2.002(16)	1.925(4)	1.966(6)	1.959(2)
Fe(2)−N(1)	2.036(5)	2.070(3)	1.976(15)	2.003(4)	1.967(6)	1.967(2)
Fe(2)−N(2)	2.037(5)	2.058(3)	1.979(15)	2.013(4)	2.004(6)	1.993(3)
Fe(2)−N(5)	2.016(5)	2.005(3)	1.984(15)	1.939(4)	1.979(7)	1.963(2)
Fe(2)−N(6)	1.981(5)	2.047(3)	1.910(15)	2.001(4)	1.925(6)	1.926(2)
Fe(3)−N(2)	2.036(5)	2.104(3)	2.017(15)	1.989(4)	2.002(6)	1.993(2)
Fe(3)−N(3)	2.037(5)	2.107(3)	1.987(15)	2.054(4)	1.987(7)	1.966(2)
Fe(3)−N(4)	2.016(5)	2.103(3)	1.980(15)	1.974(4)	1.967(6)	1.969(2)
Fe(3)−N(6)	1.981(5)	2.050(3)	2.001(15)	1.961(4)	1.929(6)	1.922(2)

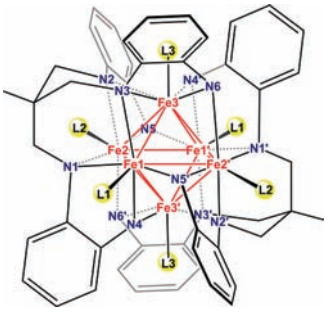

from the Fe_6 core, associated with moving from the tricationic cluster in **5** to the hexacationic cluster in **7**, results in a regular linear shift in the spectral parameters (δ, $|\Delta E_Q|$ (mm/s): 0.42, *2.52* for **5**; 0.40, *2.50* for **6**; and 0.37, *2.54* for **7**). Note that this progression corroborates our previous assignment that **7** results from a two-electron oxidation of the tetracationic cluster in **6** to form a hexacationic cluster.

The dependence of isomer shift on Fe_6 core oxidation state, depicted in Figure 6, reveals two discernible and notable trends. First, consider the clusters $[(^{H}L)_2Fe_6(L)_m]^{n+}$, where $n = -1$ to $+1$. Here, the change in isomer shift is dramatic, with a line of best fit to the three data points giving $\Delta\delta = 0.13/n$, as solvent coordination to the core is minimal (only two molecules of acetonitrile bind the cluster in **3**). In stark contrast, as the core solvates with increasing oxidation state, the change in isomer shift is more gradual, with a line of best fit to the four points corresponding to $n = 2, 3, 4$, and 6, giving $\Delta\delta = 0.014/n$, nearly an order of magnitude less steep in slope. The quadrupole splitting follows a remarkably similar trend, with $|\Delta E_Q|$ increasing with increasing oxidation of the $[Fe_6]$ core. Here, lines of best fit extracted from data analogously to those for isomer shift give $\Delta(|\Delta E_Q|) = 0.63/n$ and $0.04/n$ for $n = -1$ to $+1$ and $+2$ to $+6$, respectively.

The magnitude of change in isomer shift upon sequential oxidation from anionic cluster compound **2** to neutral **1** to cationic cluster compound **3** is similar to that observed for the one-electron oxidation of the related trinuclear core $[(^{H}L)Fe_3(PMe_2R)_3]^{n+}$ (for $n = 0$, δ, $|\Delta E_Q|$ (mm/s): 0.38, *1.03*; for $n = +1$, 0.28, *0.78*).[18] However, upon ligation of acetonitrile to the iron sites in compounds **4**−**6**, the change observed in the isomer shifts is approximately 1 order of magnitude smaller than in the trinuclear analogues, perhaps suggestive of an even greater degree of delocalization of the cationic charge through the core. Moreover, the rate of change in isomer shift in **4**−**6** is even smaller than that

dx.doi.org/10.1021/ja2015845 |*J. Am. Chem. Soc.* 2011, 133, 8293–8306

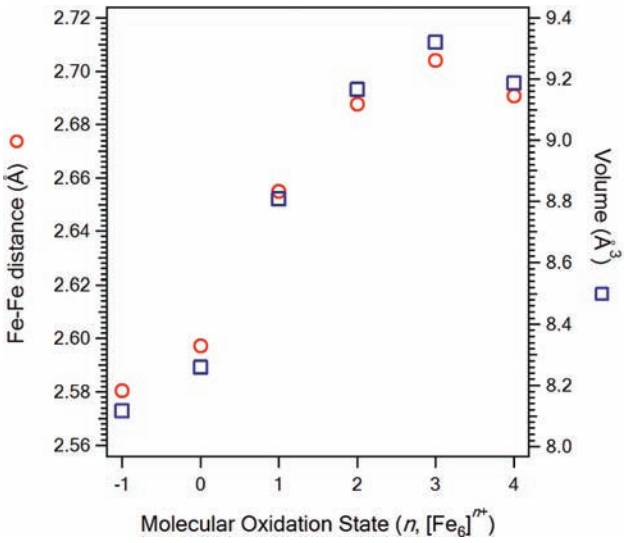

Figure 4. Modulation of Fe−Fe separation (red circles) and [Fe$_6$] core volume (blue squares) as a function of molecular oxidation state (n, [Fe$_6$]$^{n+}$).

observed for the $[Fe_6S_8(PEt_3)_6]^{n+}$ electron-transfer series, where a trend of $\Delta\delta$ = 0.14 mm/s was observed,[11r] in accordance with synthetic [Fe$_4$S$_4$] cores.[7b,34,37] In iron−sulfur clusters featuring isomer shift changes of $\Delta\delta$ < 0.06 mm/s over three oxidation states, significant ligand character contribution to the electroactive orbitals has been invoked. As such, while we have not spectroscopically or crystallographically[38] observed a perturbation in the potentially redox-active *o*-phenylenediamine ligand subunits,[39] we cannot rule out amide participation in the observed redox processes.

3.6. Magnetic Measurements. To probe the magnetic behavior of compound **1**, variable-temperature dc susceptibility data were collected under an applied dc field of 1 T in the temperature range 2−300 K. As the temperature is decreased, $\chi_M T$ undergoes a slight linear decrease from 21.2 cm^3·K/mol at 300 K to 18.2 cm^3·K/mol at 50 K. Below 50 K, $\chi_M T$ undergoes a precipitous downturn to a minimum of 5.39 cm^3·K/mol at 2 K (see Figure 7). The temperature invariance of $\chi_M T$ above 50 K is consistent with the population of an S = 6 ground state with a significant contribution from temperature-independent paramagnetism (TIP). The downturn at low temperature likely stems from a combination of Zeeman and zero-field splitting. The data were reproduced well using the program MAGPACK, according to the Hamiltonian $\hat{H} = D\hat{S}_z^2 + g_{iso}\mu_B \mathbf{S}\cdot\mathbf{H}$, considering an S = 6 ground state with g = 2.0, D = +15 cm^{-1}, and TIP = 9.0 × 10^{-3} cm^3/mol. This isolation of such a high-spin ground state up to room temperature is noteworthy. Indeed, this value represents a considerable increase over those observed for other octahedral Fe$_6$ clusters, which have previously, to our knowledge, not exceeded $S = {}^7/_2$.[11q] Considering other topologies of transition metal clusters of nuclearity greater than two, spin ground states of up to S = 4 have been observed to be isolated at room temperature.[40] Further, a number of dinuclear $Fe^{2.5}Fe^{2.5}$ complexes have been shown to exhibit $S = {}^9/_2$ ground states through double-exchange mechanisms,[41] and $Fe^{II}{}_2$ lantern species have been suggested to exhibit S = 4 ground states.[42] To our knowledge, however, the S = 6 ground state observed for **1** is the highest yet isolated at room temperature in any molecule.[19] This high-spin ground state likely arises in large part due to the weaker ligand field exerted by the amide donors in contrast to the strongly σ-donating chalcogenide or strongly π-accepting carbonyl ligands commonly found in iron clusters (see section 4 for further discussion).

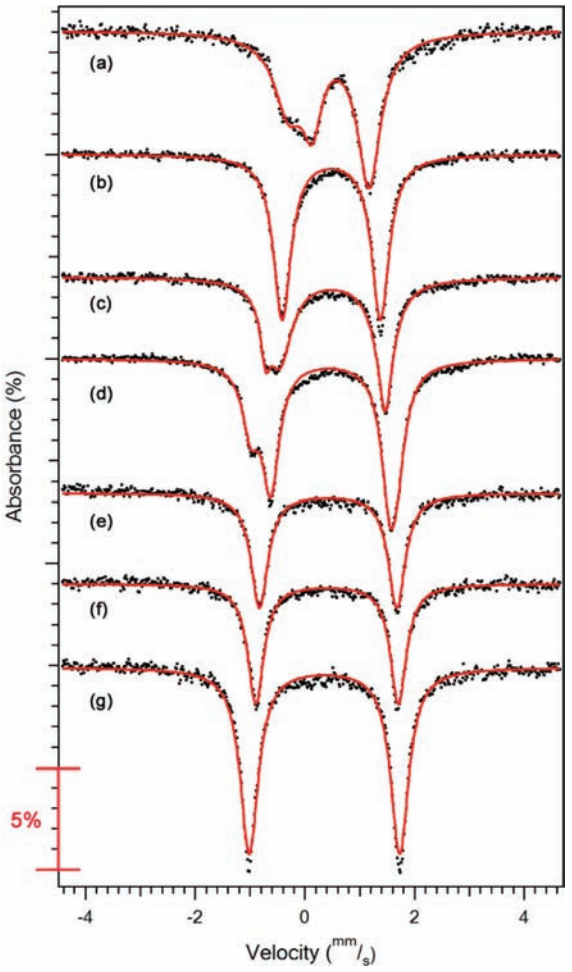

Figure 5. Zero-field, ^{57}Fe Mössbauer spectra, obtained at 100 K, for compounds **2** (a), **1** (b), **3** (c), **4** (d), **5** (e), **6** (f), and **7** (g). Solid red lines represent fits to the data.

The plot of $\chi_M T$ vs T for compound **5** shows a trend similar to that for **1**, albeit with much different values of data $\chi_M T$ (see Figure 7, inset). At 300 K, $\chi_M T$ = 1.94 cm^3·K/mol, slightly above the expected value of 1.875 cm^3·K/mol for an $S = {}^3/_2$ spin state. As the temperature is lowered, the data undergo an initially gradual decline that becomes more abrupt below 150 K. The data were modeled according to the Hamiltonian $\hat{H} = D\hat{S}_z^2 + g_{iso}\mu_B \mathbf{S}\cdot\mathbf{H}$ and the modified Van Vleck equation to give parameters of $S = {}^3/_2$, g = 2.0, $|D|$ = 76 cm^{-1}, zJ = −0.58 cm^{-1}, and TIP = 100 × 10^{-6} cm^3/mol.[43] While quite large, this value of D is in accordance with a number of mixed-valence diruthenium complexes that have been shown to exhibit a delocalized electronic structure (see below).[44] Note that the zJ term represents a mean-field approximation for interactions between neighboring clusters, where z is the number of nearest neighbors for each cluster molecule, in this case z = 6. Finally, we note that attempts to model the temperature dependence of $\chi_M T$ as superexchange between site-isolated Fe^{II} and Fe^{III} ions have failed to even remotely reproduce the experimental data.

dx.doi.org/10.1021/ja2015845 |*J. Am. Chem. Soc.* 2011, 133, 8293–8306

4. ELECTRONIC STRUCTURE CONSIDERATIONS

With a collection of structural, electrochemical, magnetic, and spectroscopic data for the electron-transfer series **1**−**7** in hand, we aim to deduce a simple electronic structure model for the Fe_6 core that accurately reflects these data. In particular, we seek to resolve the dependence of solvent-binding, structural variation of the Fe_6 core, and molecular spin state on cluster oxidation state.

4.1. Electronic Structure of $(^{H}L)_2Fe_6$. Using a delocalized M−M bonding approach derived from group theoretical considerations, akin to those used by Cotton,[45] Dahl,[46] Holm,[11q] and others[11p,47,48] to describe polynuclear metal complexes featuring close M−M ion separation, we propose a ground state configuration for **1**. First, the 12 amide nitrogen atoms and 6 Fe atoms contribute 36 and 48 valence electrons, respectively, giving a total of 84 valence electrons in the electronic structure of **1**. While the overall symmetry of **1** is formally S_6, we can treat the $[Fe_6N_{12}]$ core in local octahedral symmetry (O_h). The two $[^{H}L]^{6-}$ ligands in **1** provide 24 N-based $2p_x$ and $2p_y$ orbitals to construct the 24 σ-bonding interactions with the 6 Fe ions. The N-based σ-donor orbitals collectively transform as $(a_{1g} + a_{2g} + 2\,e_g + t_{1g} + t_{2g} + 2t_{1u} + 2t_{2u})$ and interact with the iron-based orbitals, which transform as an identical composition using the iron $3d_{x^2-y^2}$ orbitals $(a_{2g} + e_g + t_{2u})$, 4s orbitals $(a_{1g} + e_g + t_{1u})$ and 4p orbitals $(t_{1g} + t_{2g} + t_{1u} + t_{2u})$. Filling the resulting 24 bonding orbitals requires 48 of the 84 total valence electrons, creating a band of fully populated Fe−N σ-interactions, $(1a_{1g})^2(1a_{2g})^2(1e_g)^4(1t_{2u})^6(2e_g)^4(1t_{1u})^6(1t_{1g})^6(2t_{1u})^6(1t_{2g})^6(2t_{2u})^6$. The remaining 24 Fe-based 3d orbitals (d_{xy}, d_{xz}, d_{yz}, and d_{z^2}) transform as a collection of both σ and π-bonding interactions within the $[Fe_6]$ core, creating a band of bonding interactions $(a_{1g} + t_{1u} + a_{2u} + t_{2g} + t_{2g})$, a nonbonding set (e_g), and four primarily antibonding interactions $(t_{2u} + e_u + t_{1g} + t_{1u})$, ultimately giving rise to the set of frontier orbitals $(1a_{1g})(1t_{1u})(1a_{2u})(1t_{2g})(2t_{2g})(1e_g)(1t_{2u})(1e_u)(1t_{1g})(2t_{1u})$. Note that the composition of $3d_{x^2-y^2}$ orbitals $(a_{2g} + e_g + t_{2u})$ represent antibonding interactions with respect to the ligand amide nitrogen atoms ($(Fe-N)_\sigma^*$), and are thus likely too high in energy to populate. As such, these interactions will not be considered further in this analysis. Finally, populating the frontier orbitals with the remaining 36 valence electrons according to a high-spin configuration produces a band of interactions with the configuration $(a_{1g})^2(t_{1u})^6(a_{2u})^2(t_{2g})^6(t_{2g})^6(e_g)^3(t_{2u})^3(e_u)^2(t_{1g})^3(t_{1u})^3$, as illustrated in the left panel of Figure 8 (note that only the frontier Fe-based orbitals are shown). This electronic configuration predicts a spin state of $S = 6$, consistent with that extracted from the value for $\chi_M T$ data. Additionally, the consistency of a high-spin electronic configuration (neglecting $(Fe-N)_\sigma^*$ orbitals) with the experimental data highlight the importance of the weak-field ligand platform. Apparently, these interactions, in conjunction with the relatively long separation of Fe centers within the $[Fe_6]$ core, lead to an overall molecular orbital manifold

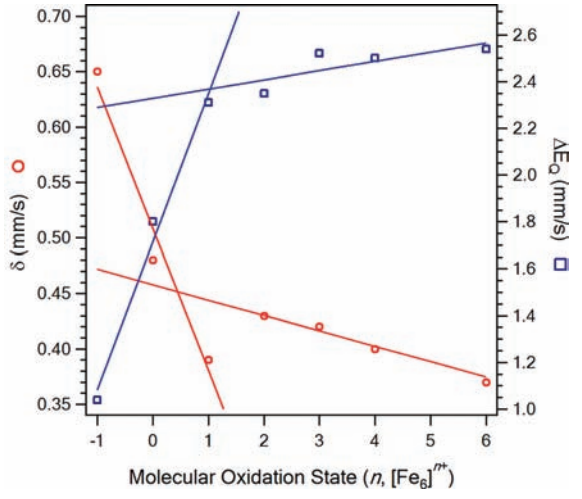

Figure 6. ^{57}Fe Mössbauer isomer shift (δ, red circles) and quadrupole splitting ($|\Delta E_Q|$, blue squares) plotted as functions of molecular oxidation state (n, $[Fe_6]^{n+}$).

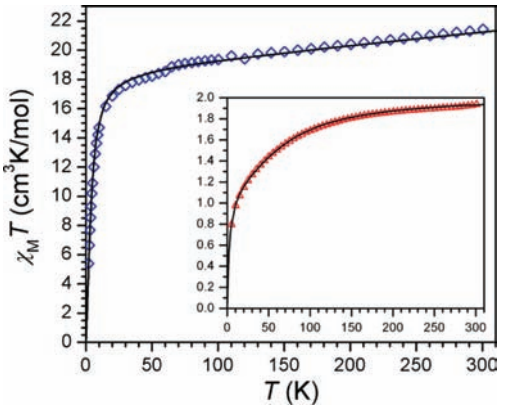

Figure 7. Variable-temperature dc magnetic susceptibility data for **1** (blue diamonds) and **5** (red triangles, inset), collected in an applied field of 1 T. Solid lines correspond to fits to the data, as described in the text. The $\chi_M T$ data are indicative of an $S = 6$ and $S = {}^3/_2$ ground state for **1** and **5**, respectively.

Table 3. Spectral and Magnetic Properties of Complexes 1−7

complex	S^a	$\chi_M T$ ($cm^3 \cdot K/mol$)^b	$E_{1/2}$ (V)	δ (mm/s)^c	$\lvert\Delta E_Q\rvert$ (mm/s)^c	(%)
$(^{H}L)_2Fe_6$ (**1**)	6	21.2	−2.04	0.48	1.79	100
$[Na(Et_2O)_2(NCMe)_2][(^{H}L)_2Fe_6]$(**2**)	$\leq {}^{11}/_2$			0.65	1.03	65
$[(^{H}L)_2Fe_6(NCMe)_2][PF_6]$ (**3**)	$\leq {}^{9}/_2$		−1.55	0.38	2.20	54
				0.50	1.93	46
$[(^{H}L)_2Fe_6(NCMe)_4][PF_6]_2$ (**4**)	≤3		−1.22	0.35	2.68	33
				0.46	2.18	67
$[(^{H}L)_2Fe_6(NCMe)_6][PF_6]_3$ (**5**)	$^3/_2$	1.9	−0.99	0.42	2.52	100
$[(^{H}L)_2Fe_6(NCMe)_6][PF_6]_4$ (**6**)	0	0^d	−0.72	0.40	2.50	100
$[(^{H}L)_2Fe_6(NCMe)_6][PF_6]_6$ (**7**)				0.37	2.54	100

^{a} Predicted by electronic structure model (see section 4). ^{b} Obtained at 300 K. ^{c} Obtained at 100 K. ^{d} Ascertained via ^{1}H NMR.

dx.doi.org/10.1021/ja2015845 |J. Am. Chem. Soc. 2011, 133, 8293–8306

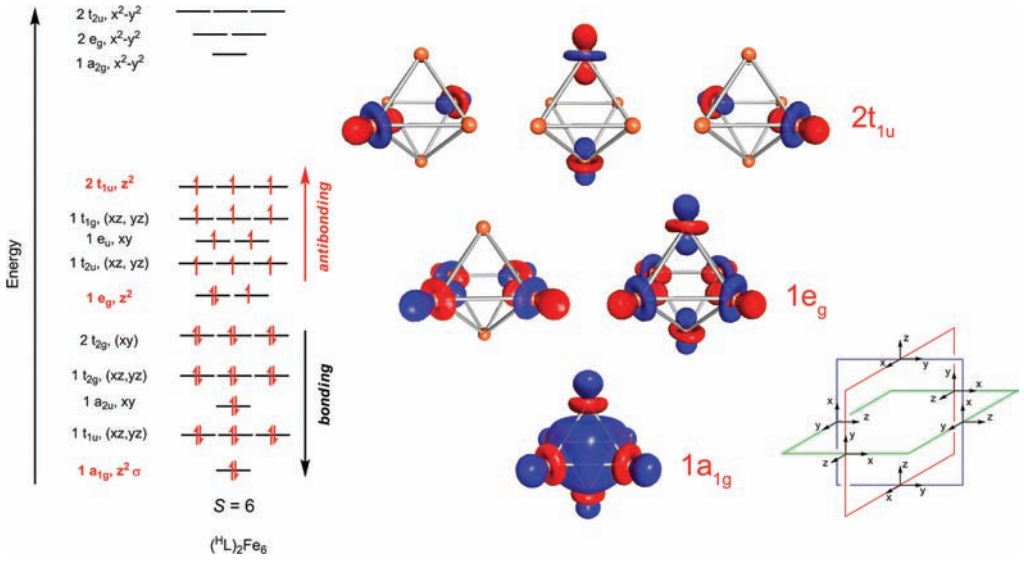

Figure 8. Left: Symmetry-allowed molecular orbital interactions comprised of the Fe 3d orbitals and electronic population $((1a_{1g})^2(1t_{1u})^6(1a_{2u})^2(1t_{2g})^6(2t_{2g})^6(1e_g)^3(1t_{2u})^3(1e_u)^2(1t_{1g})^3(2t_{1u})^3)$ to account for the $S = 6$ ground state observed for $(^{H}L)_2Fe_6$ (**1**). Right: Graphical representations for the d_{z^2} interactions are presented for the $1a_{1g}$, $1e_g$, and $2t_{1u}$ orbitals, whose electronic population dictate coordination to the $[Fe_6]$ core.

in which the energetic separation of orbitals is low enough to facilitate minimal pairing of electrons, in accordance with Hund's rules.

4.2. Electronic Structures of Electron-Transfer Series $[(^{H}L)_2Fe_6]^{n+}$. While combinations of d_{xy}, d_{xz}, and d_{yz} orbitals contribute to the σ and π interactions within the $[Fe_6]$ core, the molecular orbitals arising from linear combinations of the d_{z^2} atomic orbitals are responsible for binding of exogenous solvent ligands upon oxidation. The symmetry-adapted linear combinations (SALCs) of the six iron d_{z^2} orbitals give rise to an all in-phase, bonding interaction $(1a_{1g})^2$, a net nonbonding doubly degenerate set $(1e_g)^3$, and a triply degenerate, antibonding set $(2t_{1u})^3$ (see right panel of Figure 8 for graphical representations).[49] We note that the orbital combinations comprise the principal bonding interactions beyond the $[Fe_6]$ core and share symmetry and overall appearance with the six bonding orbital interactions experienced by a single metal ion in an octahedral field. Namely, the $1a_{1g}$ orbital is analogous to a metal s orbital, the $1e_g$ set is analogous to the $d_{x^2-y^2}$ and d_{z^2} orbitals in the e_g set, and the $2t_{1u}$ set is analogous to the p orbital set.

The position of the $2t_{1u}$ set as the highest occupied molecular orbital set in compound **1** has a significant effect on the observed reactivity upon traversing the electron-transfer series. First, consider the one-electron oxidation of **1** to the monocationic cluster in **3**. This oxidation removes an electron from the $2t_{1u}$ set and consequently engenders an unoccupied orbital with equal density at two trans-disposed Fe sites. The vacated orbital can then bind 2 equiv of acetonitrile, one at each of member of this pair of Fe sites, as observed in **3**. Next, subsequent oxidation of **3** by one electron, giving the dicationic cluster in **4**, removes a second electron from the $2t_{1u}$ set and thus enables a second trans-disposed pair of Fe centers to bind acetonitrile ligands. Finally, oxidation of **4** to **5**, resulting in a tricationic cluster, removes the third and final electron from the $2t_{1u}$ set, thereby leading to the remaining pair of trans-disposed Fe centers to bind acetonitrile ligands and giving rise to a coordinately saturated $[Fe_6]$ core.

Having developed a rationale for the dependence of acetonitrile binding on oxidation, which successfully predicts the $S = 6$ ground state experimentally observed for **1**, we turn our attention to addressing the observed core structural changes and magnetic behavior of the other clusters. While oxidation from **1** serves to remove electrons from the $2t_{1u}$ set to gate binding of solvent to the core, the previously bonding $(1a_{1g})$ and nonbonding $(1e_g)$ in-phase orbital interactions are also destabilized by these redox processes, as illustrated in Figure 9. Indeed, with each subsequent oxidation, two solvent molecules are bound, thereby destabilizing two $[Fe_6]$ core orbital interactions to nonpopulated antibonding interactions ($[Fe_6(NCMe)_n]_\sigma^*$). As a result of destabilizing these bonding and nonbonding interactions within the $[Fe_6]$ core, the number of electrons contained within the antibonding orbitals *increases* with each electron-transfer step, despite the fact the molecule is being oxidized with each electron-transfer step (see Figure 9). Thus, the total number of antibonding electrons in the $[Fe_6]$ core in the electron-transfer series sequence is 11 for compounds **1** and **3**, 12 in **4**, 13 in **5**, and 12 in **6**. Now we consider how this formulation correlates with the empirical data. The volume expansion observed for oxidation of **1** to **3** is likely due to the destabilization of the bonding interaction within the $[Fe_6]$ core as a consequence of symmetry reduction, even though the number of antibonding electrons within the core is the same (see Figure 9). In moving from **3** to **5**, the core volume expands with each subsequent oxidation, which may be a consequence of increasing electronic population of antibonding orbitals. Finally, upon oxidation of **5** to **6**, however, the Fe_6 core volume undergoes a contraction, which coincides with the decrease in antibonding electrons.[11r]

Although satisfactory magnetic susceptibility data for dicationic cluster compound **4** could not be obtained due to high reactivity, the qualitative electronic structure picture is consistent with the observed spin ground states of **1** ($S = 6$), **5** ($S = {}^3/_2$) and **6** ($S = 0$). The diamagnetism for **6** can be explained via a Jahn–Teller distortion to remove the degeneracy in the asymmetrically populated $1t_{1g}$ orbital set. The distortion allows for maximal pairing of electrons within the antibonding $[Fe_6]$ π^*-band, thereby giving rise to the ground state singlet for **6**. Although not structurally characterized, we predict the

dx.doi.org/10.1021/ja2015845 |*J. Am. Chem. Soc.* 2011, 133, 8293–8306

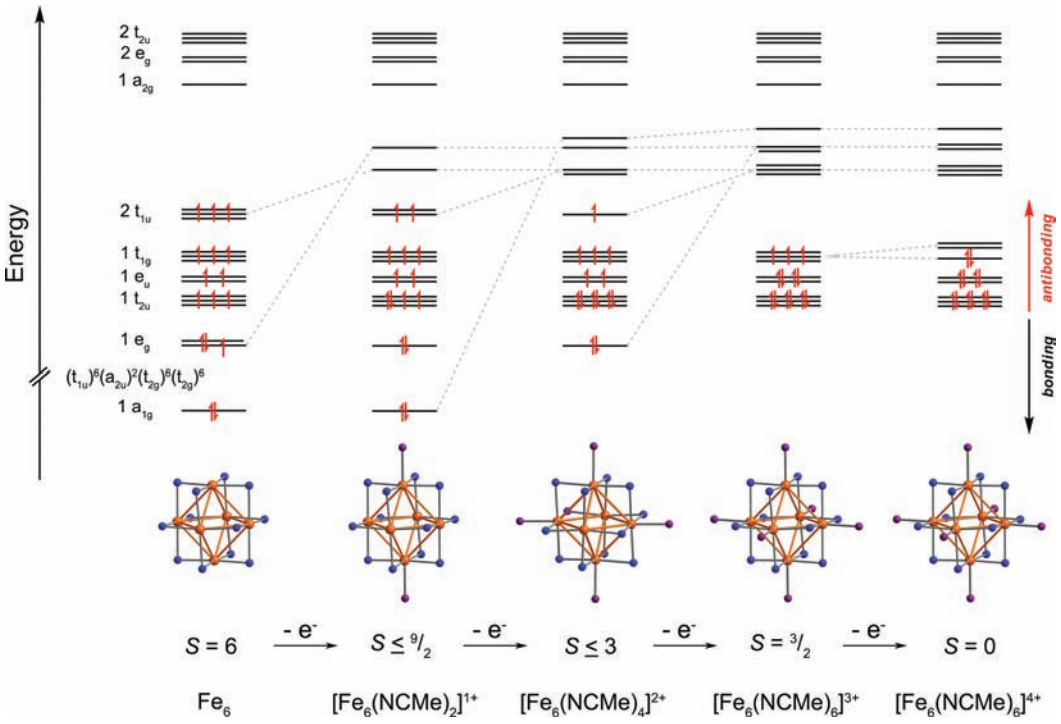

Figure 9. Proposed change in molecular orbital interactions as a function of $[Fe_6]$ core oxidation state change with the accompanying coordination number change to the $[Fe_6]$ core for the electron-transfer series represented by compound **1** and the series **3**→**6**. Ball-and-stick representations of the $[Fe_6N_{12}(NCMe)_m]$ cores are provided as a visual aid, with orange and blue spheres representing Fe and N atoms, respectively, and purple spheres representing NCMe ligands.

hexacationic (10 valence antibonding electrons) complex **7** would exhibit a core $[Fe_6]$ volume smaller than that observed in **6**.

5. CONCLUSION

The foregoing results demonstrate the ability of the hexaamide ligand $[^{H}L]^{6-}$ to direct the formation of the octahedral cluster $(^{H}L)_2Fe_6$. Cyclic voltammetric studies reveal the capacity of the $[(^{H}L)_2Fe_6]$ platform to stabilize the Fe_6 core across a range of six oxidation states. Accordingly, we are able to chemically isolate the electron-transfer series $[(^{H}L)_2Fe_6(NCMe)_m]^{n+}$ (m = 0, 2, 4, 6; n = −1, 0, 1, 2, 3, 4, 6) and structurally characterize six of these clusters. The rich electrochemistry exhibited by the cluster indicates strong electronic delocalization in the $[Fe_6]$ core, corroborated by Mössbauer spectroscopy and magnetic measurements. Moreover, the stepwise oxidation of the $[Fe_6]$ core reveals a number of fascinating observations, such as redox-directed solvent ligation and core volume flexibility. These redox-dependent properties, along with the observed spin states, provide a framework for deducing a qualitative delocalized molecular orbital picture, where the six iron centers interact to engender a set of Fe-based frontier orbitals. Taken together, these results highlight a number of exciting directions for expanding the chemistry of the $[(^{H}L)_2Fe_6]$ platform. For instance, one can envision facile modification of the hexaamide ligand to provide an even weaker-field platform, which can potentially give rise to spin states up to S = 15. In addition, work is currently underway to explore the coordination chemistry of the cluster by replacing the ancillary NCMe molecules with an array of both neutral and anionic, mono- and multitopic ligands. Such efforts will provide a means through which to perturb the electronic structure, paving the way toward new clusters and multidimensional architectures with enhanced chemical and physical properties.

■ ASSOCIATED CONTENT

Supporting Information. Crystallographic data for **1**−**6**; spectral data (ESI-MS for **1**, ^{1}H NMR for **4**−**7**) and spectral changes for the reversion of **7** to **6**; CIF files for **1**−**6**. This material is available free of charge via the Internet at http://pubs.acs.org.

■ AUTHOR INFORMATION

Corresponding Author
betley@chemistry.harvard.edu

■ ACKNOWLEDGMENT

The authors thank Harvard University for financial support, Prof. R. H. Holm for the generous use of his Mössbauer spectrometer, and the Dreyfus Environmental Postdoctoral Fellowship (Q.Z.).

■ REFERENCES

(1) (a) Peters, J. W.; Stowell, M. H. B.; Soltis, S. M.; Finnegan, M. G.; Johnson, M. K.; Rees, D. C. *Biochemistry* **1997**, *36*, 1181. (b) Mayer, S. M.; Lawson, D. M.; Gormal, C. A.; Roe, S. M.; Smith, B. E. *J. Mol. Biol.* **1999**, *292*, 871. (c) Einsle, O.; Tezcan, F. A.; Andrade, S.; Schmid, B.; Yoshida, M.; Howard, J. B.; Rees, D. C. *Science* **2002**, *297*, 1696.

(2) (a) Photosynthetic water oxidation: Special Dedicated Issue:Nugent, J., Ed. *Biochim. Biophys. Acta* **2001**, *1503*, 1. (b) Ferreira, K. N.; Iverson, T. M.; Maghlaoui, K.; Barber, J.; Iwata, S. *Science* **2004**, *303*, 1831. (c) Iwata, S.; Barber, J. *Curr. Opin. Struct. Biol.* **2004**, *14*, 447.

(3) (a) Brown, K.; Djinovic-Carugo, K.; Haltia, T.; Cabrito, I.; Saraste, M.; Moura, J. J. G.; Moura, I.; Tegoni, M.; Cambillau, C. *J. Biol. Chem.* **2000**, *275*, 41133. (b) Brown, K.; Tegoni, M.; Prudêncio, M.;

Pereira, A. S.; Besson, S.; Moura, J. J.; Moura, I.; Cambillau, C. *Nat. Struct. Biol.* **2000**, *7*, 191. (c) Chen, P.; George, S. D.; Cabrito, I.; Antholine, W. E.; Moura, J. G.; Moura, I.; Hedman, B.; Hodgson, K. O.; Solomon, E. I. *J. Am. Chem. Soc.* **2002**, *124*, 744.

(4) Siegbahn, P. E. M. *Inorg. Chem.* **2000**, *39*, 2923.

(5) (a) Fontecilla-Camps, J. C. *J. Biol. Inorg. Chem.* **1996**, *96*, 3031. (b) Huniar, U.; Ahlrichs, R.; Coucouvanis, D. *J. Am. Chem. Soc.* **2004**, *126*, 2588.

(6) Burgess, B. K.; Lowe, D. J. *Chem. Rev.* **1996**, *96*, 2983.

(7) (a) Blondin, G.; Girerd, J.-J. *Chem. Rev.* **1990**, *90*, 1359. (b) Venkateswara Rao, P.; Holm, R. H. *Chem. Rev.* **2004**, *104*, 527. (c) Lee, S. C.; Holm, R. H. *Chem. Rev.* **2004**, *104*, 1135.

(8) Selected references: M = Zr (a) Runyan, C. E., Jr.; Hughbanks, T. *J. Am. Chem. Soc.* **1994**, *116*, 7909. (b) Chen, L.; Cotton, F. A.; Wojtczak, W. A. *Inorg. Chim. Acta* **1996**, *252*, 239. (c) Chen, L.; Cotton, F. A.; Klooster, W. T.; Koetzle, T. F. *J. Am. Chem. Soc.* **1997**, *119*, 12175. (d) Xie, X.; Hughbanks, T. *Inorg. Chem.* **2002**, *41*, 1824. (e) Willems, J. B.; Rogm, H. W.; Geers, C.; Kockerling, M. *Inorg. Chem.* **2007**, *46*, 6197. M = Nb (f) Yan, B.; Zhou, H.; Lachgar, A. *Inorg. Chem.* **2003**, *42*, 8818. (g) Filed, R. A.; Kepert, D. L.; Robinson, B. W.; White, A. H. *J. Chem. Soc., Dalton Trans.* **1973**, 1858. (h) Koknat, F. W.; McCarley, R. E. *Inorg. Chem.* **1974**, *13*, 295. (i) Slougui, A.; Ouahab, L.; Perrin, C.; Grandjan, D.; Batail, P. *Acta Crystallogr., Sect. C: Cryst. Struct. Commun.* **1989**, *45*, 388. (j) Brnicevic, N.; Sirac, S.; Basic, I.; Zhang, Z.; McCarley, R. E.; Guzei, I. A. *Inorg. Chem.* **1999**, *38*, 4159. (k) Hay, D. N. T.; Swenson, D. C.; Messerle, L. *Inorg. Chem.* **2002**, *41*, 4700. M = Mo (l) Michel, J. B.; McCarley, R. E. *Inorg. Chem.* **1982**, *21*, 1864. (m) Ebihara, M.; Isobe, K.; Sasaki, Y.; Saito, K. *Inorg. Chem.* **1992**, *31*, 1644. (n) Preetz, W.; Harder, K.; von Schnering, H. G.; Kliche, G.; Peters, K. *J. Alloys Compd.* **1992**, *183*, 413. (o) Preetz, W.; Bublitz, D.; von Schnering, H. G.; Sassmanhausen, J. *Z. Anorg. Allg. Chem.* **1994**, *620*, 234. M = W (p) Penicaud, A.; Boubekeur, K.; Batail, P.; Canadell, E.; Auban-Senzier, P.; Jerome, D. *J. Am. Chem. Soc.* **1993**, *115*, 4101. (q) Gabriel, J.-C.; Boubekeur, K.; Batail, P. *Inorg. Chem.* **1993**, *32*, 2894. (r) Uriel, S.; Boubekeur, K.; Batail, P.; Orduna, J.; Canadell, E. *Inorg. Chem.* **1995**, *34*, 5307. (s) Long, J. R.; McCarty, L. S.; Holm, R. H. *J. Am. Chem. Soc.* **1996**, *118*, 4603. (t) Tulsky, E. G.; Long, J. R. *Inorg. Chem.* **2001**, *40*, 6990. M = Re (u) Zietlow, T. C.; Schaefer, W. P.; Sadeghi, B.; Hua, N.; Gray, H. B. *Inorg. Chem.* **1986**, *25*, 2195. (v) Venkataraman, D.; Rayburn, L L.; Hill, L. I.; Jin, S.; Malik, A.-S.; Turneau, J.; DiSalvo, F. J. *Inorg. Chem.* **1999**, *38*, 828. M = Cu (w) Churchill, M. R.; Bezman, S. A.; Osborn, J. A.; Wormald, J. *Inorg. Chem.* **1972**, *11*, 1818. (x) zu Kocker, R. M.; Behrendt, A.; Dehnicke, K. *Z. Naturforsch., B: Chem. Sci.* **1994**, *49*, 301. (y) zu Kocker, R. M.; Dehnicke, K.; Fenske, D. *Z. Naturforsch., B: Chem. Sci.* **1994**, *49*, 987.

(9) Dance, I.; Fisher, K. *Prog. Inorg. Chem.* **1994**, *41*, 637.

(10) Selected references: (a) Bai, G.; Roesky, H. W.; Lobinger, P.; Noltemeyer, M.; Schmidt, H.-G. *Angew. Chem., Int. Ed.* **2001**, *40*, 2156. (b) Bottomley, F.; Paez, D. E.; White, P. S. *J. Am. Chem. Soc.* **1985**, *107*, 7226. (c) Chisholm, M. H.; Heppert, J. A.; Huffman, J. C. *Polyhedron* **1984**, *3*, 475. (d) Bottomley, F.; Paez, D. E.; White, P. S. *J. Am. Chem. Soc.* **1981**, *103*, 5581. (e) Ruettinger, W. F.; Ho, D. M.; Dismukes, G. C. *Inorg. Chem.* **1999**, *38*, 1036. (f) Wong, E. L.-M.; Sun, R. W.-Y.; Chung, N. P.-Y.; Lin, C.-L. S.; Zhu, N.; Che, C.-M. *J. Am. Chem. Soc.* **2006**, *128*, 4938. (g) Ama, T.; Okamoto, K.; Yonemura, T.; Kawaguchi, H.; Takeuchi, A.; Yasui, T. *Chem. Lett.* **1997**, 1189. (h) Karmakar, A.; Sarma, R. J.; Baruah, J. B. *Polyhedron* **2007**, *12*, 1347.

(11) Selected references: M = Zr (a) Fenske, D.; Grissinger, A.; Loos, M.; Magull, J. *Z. Anorg. Allg. Chem.* **1991**, *598/599*, 121. M = Cr (b) Tsuge, K.; Imoto, H.; Soito, T. *Bull. Chem. Soc. Jpn.* **1996**, *69*, 627. (c) Hessen, B.; Siegrist, T.; Palstra, T.; Tanzler, S. M.; Steigerwald, M. L. *Inorg. Chem.* **1993**, *32*, 5165. M = Mo (d) Saito, T.; Yamamoto, N.; Imoto, H. *J. Am. Chem. Soc.* **1988**, *110*, 1646. (e) Saito, T.; Yamamoto, N.; Nagase, T.; Tsuboi, T.; Kobayashi, K.; Yamagata, T.; Imoto, H.; Unoura, K. *Inorg. Chem.* **1990**, *29*, 764. (f) Hilsensbeck, S. J.; Young, V. G., Jr.; McCarley, R. E. *Inorg. Chem.* **1994**, *33*, 1822. M = W (g) Saito, T.; Yoshikawa, A.; Yamagata, T.; Imoto, H.; Unoura, K. *Inorg. Chem.* **1989**, *28*, 3588. (h) Zhang, X.; McCarley, R. E. *Inorg. Chem.* **1995**, *34*, 2678. (i) Ehrlich, G. M.; Warren, C. J.; Vennos, D. A.; Ho, D. M.; Haushalter, R. C.; DiSalvo, F. J. *Inorg. Chem.* **1995**, *34*, 4454. (j) Jin, S.; Adamchuk, J.; Xiang, B.; DiSalvo, F. J. *J. Am. Chem. Soc.* **2002**, *124*, 9229. (k) Perruchas, S.; Flores, S.; Jousselme, B.; Lobkovsky, E.; Abruna, H.; DiSalvo, F. J. *Inorg. Chem.* **2007**, *46*, 8976. M = Re (l) Long, J. R.; McCarty, L. S.; Holm, R. H. *J. Am. Chem. Soc.* **1996**, *118*, 4603. (m) Willer, M. W.; Long, J. R.; McLauchlan, C. C.; Holm., R. H. *Inorg. Chem.* **1998**, *37*, 328. (n) Shestopalov, M. A.; Mironov, Y. V.; Brylev, K. A.; Kozlova, S. G.; Fedorov, V. E.; Spies, H.; Pietzsch, H.-J.; Stephan, H.; Geipel, G.; Bernhard, G. *J. Am. Chem. Soc.* **2007**, *129*, 3714. M = Fe (o) Cecconi, F.; Ghilardi, C. A.; Midollini, S. *Chem. Commun.* **1981**, 640. (p) Agresti, A.; Bacci, M.; Cecconi, F.; Ghilardi, C. A.; Midollini, S. *Inorg. Chem.* **1985**, *24*, 689. (q) Bencini, A.; Ghilardi, C. A.; Midollini, S.; Orlandini, A.; Russo, U.; Uytterhoeven, M. G.; Zanchini, C. *J. Chem. Soc., Dalton Trans.* **1995**, 963. (r) Goddard, C. A.; Long, J. R.; Holm, R. H. *Inorg. Chem.* **1996**, *35*, 4347. (s) Han, J.; Koutmos, M.; Al Ahmad, S.; Coucouvanis, D. *Inorg. Chem.* **2001**, *40*, 5985. (t) Steigerwald, M. L.; Siegrist, T.; Gyorgy, E. M.; Hessen, B.; Kwon, Y.-U.; Tanzler, S. M. *Inorg. Chem.* **1994**, *33*, 3389. M = Ru (u) Eckermann, A. L.; Wunder, M.; Fenske, D.; Rauchfuss, T. B.; Wilson, S. R. *Inorg. Chem.* **2002**, *41*, 2004. M = Co (v) Cecconi, F.; Ghilardi, C. A.; Midollini, S.; Orlandini, A. *Inorg. Chim. Acta* **1982**, *64*, L47.1983, *76*, L183. (w) Fenske, D.; Hachgenei, J.; Ohmer, J. *Angew. Chem., Int. Ed.* **1985**, *24*, 706. (x) Diana, E.; Gervasio, G.; Rossetti, R.; Valdemarin, F.; Bor, G.; Stanghellini, P. L. *Inorg. Chem.* **1991**, *30*, 294. (y) Bencini, A.; Ghilardi, C.; Orlandini, A.; Midollini, S.; Zanchini, C. *J. Am. Chem. Soc.* **1992**, *114*, 9898. (z) Fenske, D.; Ohmer, J.; Hacgenei, D. *Angew. Chem., Int. Ed.* **1985**, *24*, 993. (aa) Gervasio, G.; Kettle, S. F. A.; Musso, F.; Rossetti, R.; Stanghellini, P. L. *Inorg. Chem.* **1995**, *34*, 298. (ab) Steigerwald, M. L.; Sigrist, T.; Stuczynski, S. M. *Inorg. Chem.* **1991**, *30*, 2257.

(12) (a) Taft, K. L.; Caneschi, A.; Pence, L. E.; Delfs, C. D.; Papaefthymiou, G. C.; Lippard., S. J. *J. Am. Chem. Soc.* **1993**, *115*, 11753. (b) Hudson, T. A.; Berry, K. J.; Moubaraki, B.; Murray, K. S.; Robson, R. *Inorg. Chem.* **2006**, *45*, 3549. (c) Thompson, L. K. *Coord. Chem. Rev.* **2002**, *233/234*, 193. (d) Gray, T. G. *Coord. Chem. Rev.* **2003**, *243*, 213. (e) Mullins, C. S.; Pecararo, V. L. *Coord. Chem. Rev.* **2008**, *252*, 416.

(13) (a) Gall, R. S.; Connelly, N. G.; Dahl, L. F. *J. Am. Chem. Soc.* **1973**, *96*, 4017. (b) Decker, A.; Fenske, D.; Maczek, K. *Angew. Chem., Int. Ed.* **1996**, *35*, 2863. (c) Verma, A. K.; Lee, S. C. *J. Am. Chem. Soc.* **1999**, *121*, 10838. (d) Link, H.; Decker, A.; Fenske, D. *Z. Anorg. Allg. Chem.* **2000**, *626*, 1567. (e) Duncan, J. S.; Nazif, T. M.; Verma, A. K.; Lee, S. C. *Inorg. Chem.* **2003**, *42*, 1211. (f) Link, H.; Reiss, P.; Chitsaz, S.; Pfistner, H.; Fenske, D. *Z. Anorg. Allg. Chem.* **2003**, *629*, 755. (g) Lee, S. C.; Holm, R. H. *Chem. Rev.* **2004**, *104*, 1135. (h) Verma, A. K.; Nazif, T. N.; Achim, C.; Lee, S. C. *J. Am. Chem. Soc.* **2000**, *122*, 11013. (i) Krinsky, J. L.; Anderson, L. L.; Arnold, J.; Bergman, R. G. *Angew. Chem., Int. Ed.* **2007**, *46*, 309. (j) Krinsky, J. L.; Anderson, L. L.; Arnold, J.; Bergman, R. G. *Inorg. Chem.* **2008**, *47*, 1053. (k) Chen, X.-D.; Duncan, J. S.; Verma, A. K.; Lee, S. C. *J. Am. Chem. Soc.* **2010**, *132*, 15884.

(14) (a) Macchi, P.; Sironi, A. *Coord. Chem. Rev.* **2003**, *238/239*, 383. (b) King, R. B.; Bitterwolf, T. E. *Coord. Chem. Rev.* **2000**, *206/207*, 563. (c) Hughes, A. K.; Wade, K. *Coord. Chem. Rev.* **2000**, *197*, 191. (d) Xu, Q. *Coord. Chem. Rev.* **2002**, *231*, 83. (e) Ma, L.; Williams, G. K.; Shapley, J. R. *Coord. Chem. Rev.* **1993**, *128*, 261.

(15) (a) Geiger, W. E.; Connelly, N. G. *Adv. Organomet. Chem.* **1985**, *24*, 87. (b) Lemoine, P. *Coord. Chem. Rev.* **1982**, *47*, 55. (c) Drake, S. R. *Polyhedron* **1990**, *9*, 455. (d) Zanello, P. *Coord. Chem. Rev.* **1988**, *86*, 199. (e) Zanello, P. *Coord. Chem. Rev.* **1989**, *87*, 1.

(16) Selected references: (a) Mallah, T.; Auberger, C.; Verdaguer, M.; Veillet, P. *Chem. Commun.* **1995**, 61. (b) Parker, R. J.; Hockless, D. C. R.; Moubaraki, B.; Murray, K. S.; Spiccia, L. *Chem. Commun.* **1996**, 2789. (c) Zhong, Z. J.; Seino, H.; Mizobe, Y.; Hidai, M.; Fujishima, A.; Ohkoshi, S.-I.; Hashimoto, K. *J. Am. Chem. Soc.* **2000**, *122*, 2952. (d) Sokol, J. J.; Hee, A. G.; Long, J. R. *J. Am. Chem. Soc.* **2002**, *124*, 7656. (e) Berlinguette, C. P.; Vaughn, D.; Cañada-Vilalta, C.; Galán-Mascarós, J. R.; Dunbar, K. R. *Angew. Chem., Int. Ed.* **2003**, *42*, 1523. (f) Marvaud, V.; Decroix, C.; Scuiller, A.; Guyard-Duhayon, C.; Vaissermann, J.; Gonnet, F.; Verdaguer, M. *Chem.—Eur. J.* **2003**, *9*, 1677. (g) Schelter, E. J.; Prosvirin, A. V.; Dunbar,

K. R. *J. Am. Chem. Soc.* **2004**, *126*, 15004. (h) Li, D.; Parkin, S.; Wang, G.; Yee, G. T.; Prosvirin, A. V.; Holmes, S. M. *Inorg. Chem.* **2005**, *44*, 4903. (i) Ni, Z.-H.; Kou, H.-Z.; Zhang, L.-F.; Ge, C.; Cui, A.-L.; Wang, R.-J.; Li, Y.; Sato, O. *Angew. Chem., Int. Ed.* **2005**, *44*, 7742. (j) Beltran, L. M. C.; Long, J. R. *Acc. Chem. Res.* **2005**, *38*, 325. (k) Glaser, T.; Heidemeier, M.; Weyhermüller, T.; Hoffmann, R.-D.; Rupp, H.; Müller, P. *Angew. Chem., Int. Ed.* **2006**, *45*, 6033. (l) Wang, C.-F.; Zuo, J.-L.; Bartlett, B. M.; Song, Y.; Long, J. R.; You, X.-Z. *J. Am. Chem. Soc.* **2006**, *128*, 7162. (m) Harris, T. D.; Long, J. R. *Chem. Commun.* **2007**, 1360. (n) Shatruk, M.; Dragulescu Andrasi, A.; Chambers, K. E.; Stoian, S. A.; Bominaar, E. L.; Achim, C.; Dunbar, K. R. *J. Am. Chem. Soc.* **2007**, *129*, 6104. (o) Freedman, D. E.; Jenkins, D. M.; Iavarone, A. T.; Long, J. R. *J. Am. Chem. Soc.* **2008**, *130*, 2884. (p) Shatruk, M.; Avendano, C.; Dunbar, K. In *Progress in Inorganic Chemistry*; Karlin, K. D., Ed.; John Wiley & Sons: Amsterdam, 2009; Vol. 56, pp 155 and references therein. (q) Wang, X.-Y.; Prosvirin, A. V.; Dunbar, K. R. *Angew. Chem., Int. Ed.* **2010**, *122*, 5135.

(17) Selected references: (a) Fujita, M.; Yazaki, J.; Ogura, K. *J. Am. Chem. Soc.* **1990**, *112*, 5645. (b) Stang, P. J.; Cao, D. H. *J. Am. Chem. Soc.* **1994**, *116*, 4981. (c) Stang, P. J.; Cao, D. H.; Saito, S.; Arif, A. M. *J. Am. Chem. Soc.* **1995**, *117*, 6273. (d) Romero, F. M.; Ziessel, R.; Dupont-Gervais, A.; Van Dorsselaer, A. *Chem. Commun.* **1996**, 551. (e) Fujita, M.; Sasaki, O.; Mitsuhashi, T.; Fujita, T.; Yazaki, J.; Yamaguchi, K.; Ogura, K. *Chem. Commun.* **1996**, 1535. (f) Slone, R. V.; Hupp, J. T.; Stern, C. L.; Albrecht-Smith, T. E. *Inorg. Chem.* **1996**, *35*, 4096. (g) Slone, R. V.; Benkstein, K. D.; Bélanger, S.; Hupp, J. T.; Guzei, I. A.; Rheingold, A. L. *Coord. Chem. Rev.* **1998**, *171*, 221. (h) Schnebeck, R.-D.; Randaccio, L.; Zangrando, E.; Lippert, B. *Angew. Chem., Int. Ed.* **1998**, *37*, 119. (i) Cruse, H. A.; Leadbeater, N. E. *Inorg. Chem.* **1999**, *38*, 4149. (j) Bélanger, S.; Hupp, J. T.; Stern, C. L.; Slone, R. V.; Watson, D. F.; Carrell, T. G. *J. Am. Chem. Soc.* **1999**, *121*, 557. (k) Aoyagi, M.; Biradha, K.; Fujita, M. *Bull. Chem. Soc. Jpn.* **1999**, *72*, 2603. (l) Schnebeck, R.-D.; Freisinger, E.; Lippert, B. *Chem. Commun* **1999**, 675. (m) Schnebeck, R.-D.; Freisinger, E.; Lippert, B. *Eur. J. Inorg. Chem.* **2000**, 1193. (n) Schweiger, M.; Seidel, S. R.; Arif, A. M.; Stang, P. J. *Angew. Chem., Int. Ed.* **2001**, *40*, 3467. (o) Yu, X.-Y.; Maekawa, M.; Kondo, M.; Kitagawa, S.; Jin, G.-X. *Chem. Lett.* **2001**, 168. (p) Lau, V. C.; Berben, L. A.; Long, J. R. *J. Am. Chem. Soc.* **2002**, *124*, 9042. (q) Shiu, K.-B.; Lee, H.-C.; Lee, G.-H.; Ko, B.-T.; Wang, Y.; Lin, C.-C. *Angew. Chem., Int. Ed.* **2003**, *42*, 2999. (r) Kryschenko, Y. K.; Seidel, S. R.; Arif, A. M.; Stang, P. J. *J. Am. Chem. Soc.* **2003**, *125*, 5193. (s) Ferrer, M.; Mounir, M.; Rossell, O.; Ruiz, E.; Maestro, M. A. *Inorg. Chem.* **2003**, *42*, 5890. (t) Dey, S. K.; Bag, B.; Zhou, Z.; Chen, A, S, C.; Mitra, S. *Inorg. Chim. Acta* **2004**, *357*, 1991. (u) Queiroz, S. L.; Kikuti, E.; Ferreira, A. G.; Santiago, M. O.; Batista, A. A.; Castellano, E. E.; Ellena, J. *Supramol. Chem.* **2004**, *16*, 255. (v) Berben, L. A.; Faia, M. C.; Crawford, N. R. M.; Long, J. R. *Inorg. Chem.* **2006**, *45*, 6378.

(18) Zhao, Q.; Betley, T. A. *Angew. Chem., Int. Ed.* **2011**, *50*, 709.

(19) Powers, T. M.; Fout, A. R.; Zheng, S.-L.; Betley, T. A. *J. Am. Chem. Soc.* **2011**, *133*, 3336.

(20) Klose, A.; Solari, E.; Ferguson, R.; Floriani, C.; Chiesi-Villa, A.; Rizzoli, C. *Organometallics* **1993**, *12*, 2414.

(21) APEX2, v.2009; Bruker Analytical X-Ray Systems, Inc.: Madison, WI, 2009.

(22) Sheldrick, G. M. *SADABS*, Version 2.03; Bruker Analytical X-Ray Systems, Inc.: Madison, WI, 2000.

(23) Spek, A. L. *PLATON*, A Multipurpose Crystallographic Tool; Utrecht University: Utrecht, The Netherlands, 2010.

(24) Sheldrick, G. M. *SHELXTL*, Version 6.12; Bruker Analytical X-Ray Systems, Inc.: Madison, WI, 2000.

(25) (a) Evans, D. F. *J. Chem. Soc* **1959**, 2003–2005. (b) Piguet, C. *J. Chem. Educ.* **1997**, *74*, 815–816.

(26) (a) Wucherer, E. J.; Tasi, M.; Hansert, B.; Powell, A. K.; Garland, M.-T.; Halet, J.-F.; Saillard, J.-Y.; Vahrenkamp, H. *Inorg Chem.* **1989**, *28*, 3564. (b) Gao, H.-R.; Mak, T. C. W.; Kang, B.-S.; Wu, B.-M.; Xu, Y.-J.; Tong, Y.-X.; Yu, X.-L. *J. Chem. Res. S* **1996**, *5*, 186. (c) Kim, M.; Han, J. *Polyhedron* **2007**, *26*, 2949. (d) Hess, C. R.; Weyhermüller, T.; Bill, E.; Wieghardt, K. *Angew. Chem. Int. Ed.* **2009**, *48*, 3703.

(27) (a) Churchill, M. R.; Wormald, J. *J. Chem. Soc., Dalton Trans.* **1974**, 2410. (b) Gourdon, A.; Jeannin, Y. *Organometallics* **1986**, *5*, 2406. (c) Bogdan, P. L.; Sabat, M.; Sunshine, S. A.; Woodcock, C.; Shriver, D. F. *Inorg. Chem.* **1988**, *27*, 1904. (d) Pergola, R. D.; Bandini, C.; Demartin, F.; Diana, E.; Garlaschelli, L.; Stanghellini, P. L.; Zanello, P. *J. Chem. Soc., Dalton Trans.* **1996**, 747.

(28) The 2010 update of the CSD was searched (WebCSD v1.1.1) to extract data reported in this paper: webcsd.ccdc.cam.ac.uk.

(29) (a) Hegetschweiler, K.; Schmalle, H.; Streit, H. M.; Schneider, W. *Inorg. Chem.* **1990**, *29*, 3625. (b) Hegetschweiler, K.; Schmalle, H. W.; Streit, H. M.; Gramlich, V.; Hund, H.-U.; Erni, I. *Inorg. Chem.* **1992**, *31*, 1299. (c) Cornia, A.; Gatteschi, D.; Hegetschweiler, K.; Hausherr-Primo, L.; Gramlich, V. *Inorg. Chem.* **1996**, *35*, 4414. (d) Finn, R. C.; Zubieta, J. *J. Cluster Sci.* **2000**, *11*, 461. (e) Chae, H. K.; Hwang, C.; Dong, Y.; Yun, H.; Jang, H. G. *Chem. Lett.* **2000**, 992. (f) Spandl, J.; Kusserow, M.; Brudgam, I. Z. *Anorg. Allg. Chem.* **2003**, *629*, 968. (g) Jiang, G.; Bai, J.; Xing, H.; Li, Y.; You, X. *Cryst. Growth Des.* **2006**, *6*, 1264.

(30) Daniel, C.; Hartl, H. *J. Am. Chem. Soc.* **2005**, *127*, 13978.

(31) Gagne, R. R.; Spiro, C. L. *J. Am. Chem. Soc.* **1980**, *102*, 1443.

(32) (a) Fedruco, M.; Costa, D. A.; Balch, A. L.; Fawcett, W. R. *Angew. Chem., Int. Ed.* **1995**, *34*, 194. (b) Winkler, K.; Costa, D. A.; Balch, A. L.; Fawcett, W. R. *J. Phys. Chem.* **1995**, *99*, 17341. (c) Kawabe, S.; Kawai, T.; Sugimoto, R.; Yagasaki, E.; Yoshino, K. *J. Appl. Phys.* **1997**, *36*, L1055. (d) Balch, A. L.; Costa, D. A.; Winkler, K. *J. Am. Chem. Soc.* **1998**, *120*, 9614.

(33) Welch, E. J.; Crawford, N. R. M.; Bergman, R. G.; Long, J. R. *J. Am. Chem. Soc.* **2003**, *125*, 11464.

(34) (a) Downs, H. H.; Buchanan, R. M.; Pierpont, C. G. *Inorg. Chem.* **1979**, *18*, 1736. (b) McDaniel, A. M.; Tseng, H.-W.; Damrauer, N. H.; Shores, M. P. *Inorg. Chem.* **2010**, *49*, 7981.

(35) (a) Ferguson, J. A.; Meyer, T. J. *Chem. Commun.* **1971**, 623. (b) Toan, T.; Teo, B. K.; Ferguson, J. A.; Meyer, T. J.; Dahl, L. F. *J. Am. Chem. Soc.* **1977**, *99*, 408.

(36) (a) Cecconi, F.; Ghilardi, C. A.; Midollini, S.; Orlandini, A.; Zanello, P. *J. Chem. Soc., Dalton Trans.* **1987**, 831. (b) Bencini, A.; Ghilardi, C. A.; Midollini, S.; Orlandini, A.; Russo, U.; Uytterhoeven, M. G.; Zanchini, C. *J. Chem. Soc., Dalton Trans.* **1995**, 963. (c) Del Giallo, F.; Pieralli, F.; Fiesoli, L.; Spina, G. *Phys. Lett.* **1983**, *96A*, 141. (d) Bencini, A.; Uytterhoeven, M. G.; Znachini, C. *Int. J. Quantum Chem.* **1994**, *52*, 903.

(37) (a) Papaefthymiou, V.; Millar, M. M.; Münck, E. *Inorg. Chem.* **1986**, *25*, 3010. (b) Frankel, R. B.; Averill, B. A.; Holm, R. H. *J. Phys. (Paris)* **1974**, *35*, C6. (c) Evans, D. J.; Hills, A.; Hughes, D. L.; Leigh, G. J.; Houlton, A.; Silver, J. *J. Chem. Soc., Dalton Trans* **1990**, 2735. (d) Carney, M. J.; Papaethymiou, G. C.; Whitener, M. A.; Spartalian, K.; Frankel, R. B.; Holm, R. H. *Inorg. Chem.* **1988**, *27*, 346. (e) Carney, M. J.; Papaethymiou, G. C.; Spartalian, K.; Frankel, R. B.; Holm, R. H. *J. Am. Chem. Soc.* **1988**, *110*, 6084.

(38) Chaudhuri, P.; Verani, C. N.; Bill, E.; Bothe, E.; Weyhermüller, T.; Wieghardt, K. *J. Am. Chem. Soc.* **2001**, *123*, 2213.

(39) (a) Balch, A. L.; Holm, R. H. *Inorg. Chem.* **1966**, *88*, 5201. (b) Warren, L. F. *Inorg. Chem.* **1977**, *16*, 2814. (c) Anillo, A.; Diaz, M. R.; Garcia-Granda, S.; Obeso-Rosete, R.; Galindo, A.; Ienco, A.; Mealli, C. *Organometallics* **2004**, *23*, 471. (d) Bill, E.; Bothe, E.; Chaudhuri, P.; Chlopek, K.; Herebian, K.; Kokatam, S.; Ray, K.; Weyhermüller, T.; Neese, F.; Wieghardt, K. *Chem.—Eur. J.* **2005**, *11*, 204. (e) Chlopek, K.; Bill, E.; Weyhermüller, T.; Wieghardt, K. *Inorg. Chem.* **2005**, *44*, 7087.

(40) Chakrabarti, M.; Deng, L.; Holm, R. H.; Münck, E.; Bominaar, E. L. *Inorg. Chem.* **2009**, *48*, 2735.

(41) Selected references: (a) Drüeke, S.; Chaudhuri, P.; Pohl, K.; Wieghardt, K.; Ding, X.-Q.; Bill, E.; Sawaryn, A.; Trautwein, A. X.; Winkler, H.; Gurman, S. J. *Chem. Commun.* **1989**, 59. (b) Ding, X.-Q.; Bominaar, E. L.; Bill, E.; Winkler, H.; Trautwein, A. X.; Drüeke, S.; Chaudhuri, P.; Wieghardt, K. *J. Chem. Phys.* **1990**, *92*, 178. (c) Beissel, T.; Birkelbach, F.; Bill, E.; Glaser, T.; Kesting, F.; Krebs, C.; Weyhermüller,

T.; Wieghardt, K.; Butzlaff, C.; Trautweinet, A. X. *J. Am. Chem. Soc.* **1996**, *118*, 12376. (d) Dutta, S. K.; Ensling, J.; Werner, R.; Flörke, U.; Haase, W.; Gütlich, P.; Nag, K. *Angew. Chem., Int. Ed.* **1997**, *36*, 152. (e) LeCloux, D. D.; Davydov, R.; Lippard, S. J. *J. Am. Chem. Soc.* **1998**, *120*, 6810. (f) Lee, D.; Krebs, C.; Huynh, B. H.; Hendrich, M. P.; Lippard, S. J. *J. Am. Chem. Soc.* **2000**, *122*, 5000.

(42) (a) Cotton, F. A.; Daniels, L. M.; Matonic, J. H.; Murillo, C. A. *Inorg. Chim. Acta* **1997**, *256*, 277. (b) Cotton, F. A.; Daniels, L. M.; Falvello, L. R.; Matonic, J. H.; Murillo, C. A. *Inorg. Chim. Acta* **1997**, *256*, 269.

(43) The $\chi_M T$ vs T data were fit to the Van Vleck equation, modified to include a zJ term that describes interactions between neighboring clusters according to a mean-field approximation, as follows:

$$\chi_M = \frac{\chi \mathrm{Fe}_6}{\left(1 - \frac{2zJ}{Ng^2{\mu_B}^2}\right)\chi \mathrm{Fe}_6} + \chi_{TIP}$$

$$\chi \mathrm{Fe}_6 = \frac{\chi_z + 2\chi_x}{3}$$

$$\chi_z = \frac{Ng^2{\mu_B}^2}{4k_BT}\,\frac{1 + 9e^{-2A}}{1 + e^{-2A}}$$

$$\chi_x = \frac{Ng^2{\mu_B}^2}{k_BT}\,\frac{1 + (3/4A)(1 - e^{-2A})}{1 + e^{-2A}}$$

$$A = \frac{D}{k_BT}$$

See: Ababei, R.; Li, Y.-G.; Roubeau, O.; Kalisz, M.; Bréfuel, N.; Coulon, C.; Harté, E.; Liu, X.; Mathonière, C.; Clérac, R. *New J. Chem.* **2009**, *33*, 1237.

(44) (a) Telser, J.; Drago, R. S. *Inorg. Chem.* **1984**, *23*, 3114. (b) Telser, J.; Drago, R. S. *Inorg. Chem.* **1985**, *24*, 4765. (c) Cukiernik, F. D.; Giroud-Godquin, A. M.; Maldivi, P.; Marchon, J. C. *Inorg. Chim. Acta* **1994**, *215*, 203. (d) Handa, M.; Sayama, Y.; Mikuriya, M.; Nukada, R.; Hiromitsu, I.; Kasuga, K. *Bull. Chem. Soc. Jpn.* **1998**, *71*, 119. (e) Jimenez-Aprariclo, R.; Urbanos, F. A.; Arrieta, J. M. *Inorg. Chem.* **2001**, *40*, 613. (f) Vos, T. E.; Liao, Y.; Shum, W. W.; Her, J.-H.; Stephens, P. W.; Reiff, W. M.; Miller, J. S. *J. Am. Chem. Soc.* **2004**, *126*, 11630.

(45) Cotton, F. A.; Haas, T. E. *Inorg. Chem.* **1964**, *3*, 10.

(46) (a) Foust, A. S.; Dahl, L. F. *J. Am. Chem. Soc.* **1970**, *92*, 7337. (b) Simon, G. L.; Dahl, L. F. *J. Am. Chem. Soc.* **1973**, *95*, 2164. (c) Simon, G. L.; Dahl, L. F. *J. Am. Chem. Soc.* **1973**, *95*, 2175. (d) Chu, C. T.-W.; Gall, R. S.; Dahl, L. F. *J. Am. Chem. Soc.* **1982**, *104*, 737.

(47) Johansson, G.; Lipscomb, W. N. *Acta Crystallogr.* **1958**, *11*, 594.

(48) Hoffman, G. G.; Bashkin, J. K.; Karplus, M. *J. Am. Chem. Soc.* **1990**, *112*, 8705.

(49) Graphics were generated using TurboMole. (a) *TURBOMOLE*, V6.2, 2010; a development of U. Karlsruhe and Forschungszentrum Karlsruhe GmbH, 1989−2007 (www.turbomole.com). (b) Ahlrichs, R.; Bär, M.; Häser, M.; Horn, H.; Kölmel, C. *Chem. Phys. Lett.* **1989**, *162*, 165.